PHYSICAL REVIEW B **87**, 245107 (2013)

Reduced density matrix after a quantum quench

Maurizio Fagotti and Fabian H. L. Essler
The Rudolf Peierls Centre for Theoretical Physics, Oxford University, Oxford, OX1 3NP, United Kingdom
(Received 9 March 2013; published 12 June 2013)

We consider the reduced density matrix (RDM) $\rho_A(t)$ for a finite subsystem A after a global quantum quench in the infinite transverse-field Ising chain. It has been recently shown that the infinite time limit of $\rho_A(t)$ is described by the RDM $\rho_{\mathrm{GGE},A}$ of a generalized Gibbs ensemble. Here, we present some details on how to construct this ensemble in terms of *local* integrals of motion, and show its equivalence to the expression in terms of mode occupation numbers widely used in the literature. We then address the question of how $\rho_A(t)$ approaches $\rho_{\mathrm{GGE},A}$ as a function of time. To that end, we introduce a distance on the space of density matrices and show that it approaches zero as a universal power law $t^{-3/2}$ in time. As the RDM completely determines all local observables within A, this provides information on the relaxation of correlation functions of local operators. We then address the issue of how well a truncated generalized Gibbs ensemble with a finite number of local higher conservation laws describes a given subsystem at late times. We find that taking into account only local conservation laws with a range at most comparable to the subsystem size provides a good description. However, excluding even a single one of the most local conservation laws in general completely spoils this agreement.

DOI: 10.1103/PhysRevB.87.245107 PACS number(s): 75.10.Pq, 02.30.Ik, 03.67.Mn, 67.85.−d

I. INTRODUCTION

Recent advances in systems of optically trapped ultracold atomic gases have made it possible to observe the nonequilibrium time evolution of isolated many particle systems over long time scales.[1–6] A key property of such cold atomic clouds is their weak coupling to the environment and resulting smallness of external dissipative processes. To a good approximation, one is dealing with isolated quantum mechanical many particle systems, which are prepared in generally mixed states, and one is interested in the time dependence of observables, in particular at late times. The experimental results have stimulated theoretical efforts aimed at understanding the principles underlying the nonequilibrium dynamics of isolated many particle systems. Some of the most basic questions are whether observables generally relax to time-independent values and, if they do, whether their stationary values are described by a statistical ensemble. Other prominent issues concern the roles of dimensionality and conservations laws. Experiments on trapped ^{87}Rb atoms[2] established that three-dimensional condensates rapidly relax to a stationary state characterized by an effective temperature, whereas constraining the motion of atoms to one dimension leads to a much slower relaxation to a nonthermal distribution. It was argued that this observed difference has its origin in the presence of additional (approximate) conservation laws, related to quantum integrability, in the one-dimensional case. Theoretical efforts aimed at understanding these and related questions[7–45] indicate that in translationally invariant models there are at least two basic types of behaviors at late times: subsystems either thermalize,[46] i.e., are characterized by a Gibbs distribution with an effective temperature, or they are described by a generalized Gibbs ensemble (GGE).[8] There is evidence that the latter applies to integrable models, while the former constitutes the "generic" situation.

A popular protocol for analyzing nonequilibrium evolution is a so-called *quantum quench*: here the system is originally prepared in the ground state $|\Psi_0\rangle$ of some local, short ranged Hamiltonian $H(h_0)$, where h_0 is a system parameter such as a magnetic field or an interaction strength. At time $t=0$, h_0 is then suddenly "quenched" to h, and the subsequent time evolution under the new Hamiltonian $H(h)$ is studied. Under this protocol the system remains in a pure state $|\Psi_t\rangle = \exp[-iH(h)t]|\Psi_0\rangle$ at all times, and as a whole can clearly never be described by a Gibbs or generalized Gibbs distribution. This can be seen by considering the Hermitian operators

$$\mathcal{O}^{(n,m)} = |n\rangle\langle m| + |m\rangle\langle n|, \tag{1.1}$$

where $|n\rangle$ and $|m\rangle$ are eigenstates of $H(h)$ with energies E_n and E_m, respectively. Then the expectation values

$$\langle\Psi_t|\mathcal{O}^{(n,m)}|\Psi_t\rangle = \langle\Psi_0|n\rangle\langle m|\Psi_0\rangle e^{i(E_n-E_m)t} + \text{H.c.} \tag{1.2}$$

are oscillating in time and never become stationary. A useful and intuitive point of view is to focus on *local* properties of a given system in the thermodynamic limit, i.e., ask questions only about observables contained in a finite subsystem A.[13,31,32] Here, the (infinitely large) complement $\bar{A}$ of A can act as an effective bath, and probability may freely dissipate from A to $\bar{A}$. As a result A may be described by a mixed state. Arguably the most precise and convenient description of this situation is in terms of the reduced density matrix $\rho_A(t)$ of subsystem A. The latter is obtained from the density matrix $\rho(t) = |\Psi_t\rangle\langle\Psi_t|$ of the entire system as

$$\rho_A(t) = \mathrm{Tr}_{\bar{A}}\left[\rho(t)\right]. \tag{1.3}$$

A central question is then whether for any finite subsystem A

$$\lim_{t\to\infty} \rho_A(t) = \rho_{\mathrm{stat},A}, \tag{1.4}$$

where $\rho_{\mathrm{stat},A}$ is a time-independent reduced density matrix obtained as

$$\rho_{\mathrm{stat},A} = \mathrm{Tr}_{\bar{A}}\left[\rho_{\mathrm{stat}}\right]. \tag{1.5}$$

If (1.4) holds, then the system evolves towards a stationary state described by the distribution ρ_{stat}. In particular, (1.4) implies that the expectation values of *any* local operator $\mathcal{O}_A$

acting only within subsystem A are given by

$$\lim_{t\to\infty}\langle\Psi_t|\mathcal{O}_A|\Psi_t\rangle = \mathrm{Tr}\,[\rho_{\rm stat}\,\mathcal{O}_A]\,. \tag{1.6}$$

An efficient way of investigating whether a given RDM approaches a known stationary distribution at late times was introduced in Ref. 20 by considering the operator norm $\|\,\rho_A(t)-\rho_{{\rm stat},A}\,\|_{\rm op}$. If this approaches zero at late times, then the system relaxes locally to the stationary distribution $\rho_{\rm stat}$. Reference 20 was concerned with the case where $\rho_{\rm stat}$ describes a thermal ensemble with a given effective temperature, and considered very small subsystems. Here, we are interested in a quench to a quantum integrable model. As we have alluded to before, the stationary state for such quenches is believed to be described locally by a generalized Gibbs ensemble (for the model we consider below this was established in Ref. 32). More precisely, the density matrix of the entire system is expected to be of the form

$$\rho_{\rm stat}=\rho_{\rm GGE}=\frac{1}{\mathcal{Z}}e^{-\sum_n\lambda_n I_n}, \tag{1.7}$$

where Z is a normalization[47] and I_n are *local* conserved quantities, operators with local densities such that

$$[I_n,I_m]=0=[I_m,H(h)]. \tag{1.8}$$

The Lagrange mutipliers λ_n are fixed by the requirements

$$\langle\Psi_0|I_n|\Psi_0\rangle=\mathrm{Tr}\,[\rho_{\rm GGE}I_n]\,. \tag{1.9}$$

We stress that the GGEs considered in the quench context are fundamentally different from thermal ensembles because through the specific values of the Lagrange multipliers they retain an infinite amount of information about the initial state. Above, we have stipulated that only local (in space) conservation laws I_n are to be included in the definition of $\rho_{\rm GGE}$, but it is in fact a matter of ongoing debate as to whether locality is a necessary or even desirable requirement.[48] In this context, a result obtained in Ref. 31 is rather illuminating: there it was demonstrated for a particular example, the transverse-field Ising chain, that different statistical ensembles can have identical local properties. The two ensembles considered were a GGE of the form (1.7), and the so-called "pair ensemble" obtained by time averaging the quench density matrix $\rho(t)$. Given that $\rho_{\rm stat}$ is generally not unique, it is clearly desirable to identify the simplest description. To that end, we introduce *truncated generalized Gibbs ensembles* of the form

$$\rho^{(n_0)}_{\rm tGGE}=\frac{1}{\mathcal{Z}}e^{-\sum_{n<n_0}\lambda_n I_n}, \tag{1.10}$$

and investigate how well such ensembles describe the stationary state for quenches to integrable models.

The outline of this paper is as follows. In Sec. II we review some relevant results for the transverse-field Ising chain. Local conservation laws are presented in Sec. III and used in Secs. IV, V, and VI to define several classes of generalized Gibbs ensembles. Properties of corresponding reduced density matrices are discussed in Sec. VII. In Sec. VIII we discuss general properties of distances on the space of reduced density matrices and introduce the distance used in the remainder of the paper. In Secs. IX, X, XI, and XII we present results for the distance between quench and generalized Gibbs reduced density matrices. We summarize our results in Sec. XIII. Various technical issues are discussed in four Appendices.

II. SOME FACTS ABOUT THE TRANSVERSE-FIELD ISING CHAIN (TFIC)

Here we briefly review some relevant results on the TFIC. The latter is an important paradigm for quantum phase transitions in equilibrium[49] as well as nonequilibrium dynamics.[14,24,29,31,32,36,50] In the latter context, experimental realizations range from cold atomic gases[51] to circuit QED.[52] The Hamiltonian of the model on a ring is

$$H(h)=-J\sum_{j=1}^{L}\left[\sigma_j^x\sigma_{j+1}^x+h\sigma_j^z\right], \tag{2.1}$$

where $\sigma^\alpha_{L+1}=\sigma^\alpha_1$. The quantum spins can be mapped to (real) Majorana fermions by means of the Jordan-Wigner transformation

$$a_{2\ell}=\left(\prod_{j=1}^{\ell-1}\sigma_j^z\right)\sigma_\ell^y\,,\quad a_{2\ell-1}=\left(\prod_{j=1}^{\ell-1}\sigma_j^z\right)\sigma_\ell^x\,, \tag{2.2}$$

where $\{a_i,a_j\}=2\delta_{ij}$. In terms of the Majorana fermions (2.2), the Hamiltonian takes a block-diagonal form

$$\begin{aligned}H(h)&=\frac{1+e^{i\pi\mathcal{N}}}{2}H_{\rm R}+\frac{1-e^{i\pi\mathcal{N}}}{2}H_{\rm NS},\\ H_{\rm NS/R}&=iJ\sum_{j=1}^{L-1}a_{2j}[a_{2j+1}-ha_{2j-1}]-iJa_{2L}[ha_{2L-1}\mp a_1].\end{aligned} \tag{2.3}$$

Here, $\mathcal{N}$ is the number operator

$$\mathcal{N}=\sum_{j=1}^{L}\frac{\sigma_j^z-1}{2}=\sum_{j=1}^{L}\frac{ia_{2j}a_{2j-1}-1}{2}, \tag{2.4}$$

and by construction $e^{i\pi\mathcal{N}}=\prod_j\sigma_j^z$ commutes with $H_{\rm R,NS}$. The two blocks $H_{\rm R}$ and $H_{\rm NS}$ correspond to periodic and antiperiodic boundary conditions on the fermions, respectively. They can be diagonalized by Bogoliubov transformations

$$\begin{aligned}a_{2j-1}&=\frac{1}{\sqrt{L}}\sum_p e^{i\frac{\theta_p}{2}-ipj}[\alpha_p+\alpha^\dagger_{-p}],\\ a_{2j}&=-\frac{i}{\sqrt{L}}\sum_p e^{-i\frac{\theta_p}{2}-ipj}[\alpha_p-\alpha^\dagger_{-p}],\end{aligned} \tag{2.5}$$

where the Bogoliubov angle θ_p is given by

$$e^{i\theta_p}=\frac{h-e^{ip}}{\sqrt{1+h^2-2h\cos p}}. \tag{2.6}$$

The diagonal form of the Hamiltonian is

$$H_{\rm NS}(h)=\sum_{p\in{\rm NS}}\varepsilon_h(p)\left(\alpha_p^\dagger\alpha_p-\frac{1}{2}\right), \tag{2.7}$$

where the single-particle energy is given by

$$\varepsilon_h(k)=2J\sqrt{1+h^2-2h\cos k}. \tag{2.8}$$

The ground states of $H_{\rm R,NS}(h)$ are the fermionic vacua

$$\alpha_p|0;h\rangle_{\rm R,NS}=0\,. \tag{2.9}$$

Here, the momenta are $p = \frac{\pi n}{L}$, where n are even/odd integers for R and NS fermions, respectively.

A. Quantum quenches

Our quench protocol is as follows: we prepare the system in the ground state $|\Psi_0\rangle$ for an initial value h_0 of the transverse magnetic field. At time $t = 0$ we instantaneously change the field from h_0 to h. The state of the system at times $t > 0$ is obtained by evolving with respect to the new Hamiltonian $H(h)$:

$$|\Psi_t\rangle = e^{-iH(h)t}|\Psi_0\rangle. \tag{2.10}$$

An important quantity is the difference $\Delta_k = \theta_k - \theta_k^0$ of Bogoliubov angles required to diagonalize $H(h)$ and $H(h_0)$, respectively,

$$\cos\Delta_k = \frac{4J^2[1 + hh_0 - (h + h_0)\cos k]}{\varepsilon_h(k)\varepsilon_{h_0}(k)}. \tag{2.11}$$

As we are interested in obtaining results in the thermodynamic limit, we have to distinguish between two cases.

1. Quenches from the paramagnetic phase $h_0 > 1$

Here the initial state in a large, finite volume is simply the NS vacuum

$$|\Psi_0\rangle = |0;h_0\rangle_{\rm NS}. \tag{2.12}$$

The time evolved state can then be written in the form[31]

$$|\Psi_t\rangle = \frac{1}{\mathcal{M}}\exp\left[i\sum_{0<p\in{\rm NS}}\tan\left(\frac{\Delta_p}{2}\right)e^{-2i\varepsilon_p t}\alpha^\dagger_{-p}\alpha^\dagger_p\right]|0;h\rangle_{\rm NS}, \tag{2.13}$$

where $|0;h\rangle_{\rm NS}$ is the ground state of $H_{\rm NS}(h)$ and $\mathcal{M}$ a normalization factor.

2. Quenches from the ferromagnetic phase $h_0 < 1$

Here our initial state in a large, finite volume must reflect the spontaneous symmetry breaking of the $\mathbb{Z}_2$ spin-flip symmetry $\sigma^{x,y} \to -\sigma^{x,y}$ in the thermodynamic limit. The appropriate choice is[31]

$$|\Psi_0\rangle = \frac{|0;h_0\rangle_{\rm R} + |0;h_0\rangle_{\rm NS}}{\sqrt{2}}. \tag{2.14}$$

III. LOCAL CONSERVATION LAWS IN THE TFIC

We consider the one-dimensional transverse-field Ising chain in the thermodynamic limit

$$H = -J\sum_{n=-\infty}^{\infty}\sigma_n^x\sigma_{n+1}^x + h\sigma_n^z. \tag{3.1}$$

Following Ref. 53 we can construct an infinite number of *local* conservation laws $I_n^\pm$,

$$\left[I_n^\alpha, I_m^\beta\right] = 0, \quad n = 0,1,\ldots,\alpha,\beta = \pm, \tag{3.2}$$

where the Hamiltonian itself is $H = I_0^+$. Let us define operators

$$\begin{aligned} U_{n>0} &= \frac{1}{2}\sum_{j=-\infty}^{\infty}\sigma_j^x\left(\prod_{l=1}^{n-1}\sigma_{j+l}^z\right)\sigma_{j+n}^x,\\ U_0 &= -\frac{1}{2}\sum_{j=-\infty}^{\infty}\sigma_j^z,\\ U_{n<0} &= \frac{1}{2}\sum_{j=-\infty}^{\infty}\sigma_j^y\left(\prod_{l=1}^{|n|-1}\sigma_{j+l}^z\right)\sigma_{j+|n|}^y \end{aligned} \tag{3.3}$$

and

$$\begin{aligned} V_{n>0} &= \frac{1}{2}\sum_{j=-\infty}^{\infty}\sigma_j^x\left(\prod_{l=1}^{n-1}\sigma_{j+l}^z\right)\sigma_{j+n}^y,\\ V_{n<0} &= -\frac{1}{2}\sum_{j=-\infty}^{\infty}\sigma_j^y\left(\prod_{l=1}^{|n|-1}\sigma_{j+l}^z\right)\sigma_{j+|n|}^x. \end{aligned} \tag{3.4}$$

In terms of these operators the local conservation laws are

$$\begin{aligned} I_n^+ &= -J(U_{n+1} + U_{1-n}) + hJ(U_n + U_{-n}),\\ I_n^- &= J(V_{n+1} + V_{-n-1}), \quad n \geqslant 0. \end{aligned} \tag{3.5}$$

They are local in the sense that the density of I_n^α involves only spins on $n + 2$ neighboring sites. By virtue of their locality, the conservation laws can all be expressed in terms of Jordan-Wigner fermions (2.2):

$$\begin{aligned} I_n^+ &= \frac{i}{2}\sum_{j=-\infty}^{\infty}Ja_{2j}[a_{2j+2n+1} + a_{2j-2n+1}]\\ &\quad - hJa_{2j}[a_{2j+2n-1} + a_{2j-2n-1}],\\ I_{n-1}^- &= -\frac{iJ}{2}\sum_{j=-\infty}^{\infty}a_{2j}a_{2j+2n} + a_{2j-1}a_{2j+2n-1}. \end{aligned} \tag{3.6}$$

We now realize that all conservation laws (3.6) are in fact quadratic in Majorana fermions! It is then a simple matter to diagonalize them simultaneously by means of a Bogoliubov transformation (2.5), where on the infinite chain the Bogoliubov fermion operators have anticommutation relations

$$\{\alpha_p, \alpha_k^\dagger\} = 2\pi\delta(p - k). \tag{3.7}$$

The conservation laws take the simple form

$$\begin{aligned} I_n^+ &= \int_{-\pi}^{\pi}\frac{dk}{2\pi}\cos(nk)\varepsilon_h(k)\alpha_k^\dagger\alpha_k,\\ I_n^- &= -\int_{-\pi}^{\pi}\frac{dk}{2\pi}2J\sin[(n+1)k]\alpha_k^\dagger\alpha_k, \end{aligned} \tag{3.8}$$

which furthermore shows that they are even/odd under spatial reflections. Interestingly the conservation laws I_n^- do not depend on the transverse field h and are therefore *shared* by the entire one-parameter family of Hamiltonians $H(h)$. This seems to be a generic feature of models with a free fermion spectrum like the TFIC (see Appendix C and Ref. 59).

A. Local conservation laws for periodic boundary conditions

Above we focused on the bulk contribution to the local conservation laws. For a finite system on a ring there are boundary contributions, which can be determined as follows. In terms of the Bogoliubov fermions, the conservation laws for periodic boundary conditions are

$$I_n^+ = \sum_k \cos(nk)\varepsilon(k)\alpha_k^\dagger\alpha_k,$$
$$I_n^- = -\sum_k 2J\sin[(n+1)k]\alpha_k^\dagger\alpha_k, \tag{3.9}$$

where the momenta are taken to be either in the R or NS sectors. By inverting the Bogoliubov transformation and Fourier transforming back to position space, one obtains a representation of the conservation laws in terms of the Majorana fermions a_j for periodic/antiperiodic boundary conditions, respectively. Finally, inverting the Jordan-Wigner transformation gives the desired expression in terms of spins.

IV. GENERALIZED GIBBS ENSEMBLE

We now *define* the density matrix of a generalized Gibbs ensemble formally by the expression

$$\rho_{\rm GGE} = \frac{1}{\mathcal{Z}}\exp\left(-\sum_{n=0}^{\infty}\sum_{\sigma=\pm}\left[\lambda_n^\sigma I_n^\sigma\right]\right), \tag{4.1}$$

where $\mathcal{Z}$ is a normalization that ensures $\mathrm{Tr}\rho_{\rm GGE} = 1$. In practice we need to regularize (4.1) in an asymptotically large, finite volume L.

The Lagrange multipliers λ_n^σ are fixed through the requirements

$$\lim_{L\to\infty}\frac{1}{L}\mathrm{Tr}\left[\rho_{\rm GGE}I_n^\sigma\right] = \lim_{L\to\infty}\frac{\langle\Psi_0|I_n^\sigma|\Psi_0\rangle}{L}. \tag{4.2}$$

Using translational invariance we can alternatively work with the densities of the conservation laws

$$I_n^\sigma = \sum_{j=-\infty}^{\infty}\left(I_n^\sigma\right)_{j,\dots,j+n+1} \tag{4.3}$$

to rewrite (4.2) as

$$\mathrm{Tr}\left[\rho_{\rm GGE}\left(I_n^\sigma\right)_{j,\dots,j+n+1}\right] = \langle\Psi_0|\left(I_n^\sigma\right)_{j,\dots,j+n+1}|\Psi_0\rangle. \tag{4.4}$$

The solution to this system of equations is

$$\lambda_l^+ = (2-\delta_{l,0})\int_{-\pi}^{\pi}\frac{dk}{\pi}\frac{\cos(lk)}{\varepsilon_h(k)}\mathrm{arctanh}(\cos\Delta_k), \quad \lambda_l^- = 0, \tag{4.5}$$

where $l \geqslant 0$ and $\cos\Delta_k$ is defined in (2.11). In Fig. 1 we show λ_l^+ for a quench from $h_0 = 0.1$ to $h = 0.7$. The large l behavior of Eq. (4.5) is determined by the regions $k \sim 0,\pi$ (where the integrand has a logarithmic singularity) and one can show that

$$\lambda_l^+ \sim \frac{2}{l}\left(\pm\frac{1}{\varepsilon_h(0)} + \frac{(-1)^l}{\varepsilon_h(\pi)}\right), \tag{4.6}$$

where the sign is $+$ for quenches within the same phase and $-$ otherwise. We see that the Lagrange multipliers λ_n^+ decay rather slowly as a function of n.

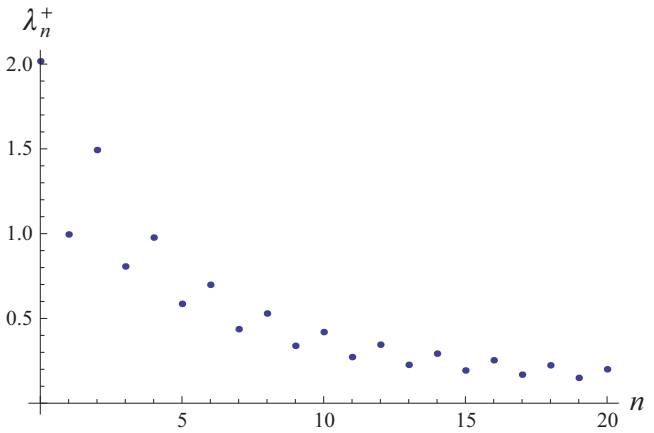

FIG. 1. (Color online) Parameters λ_n for a quench within the ordered phase from $h_0 = 0.1$ to $h = 0.7$.

A. GGE in terms of mode occupation numbers

In the literature, the generalized Gibbs ensemble is often constructed from mode occupation numbers $n_k = \alpha_k^\dagger\alpha_k$ (see, e.g., Refs. 8, 12, 18, 54, and 55). The latter are nonlocal (in space) as they involve a Fourier transform. We will now establish the relation between this and our definition (4.1). It follows from (3.8) that the density matrix can be rewritten in the form

$$\rho_{\rm GGE} = \frac{1}{\mathcal{Z}}\exp\left(-\int_{-\pi}^{\pi}\frac{dk}{2\pi}\gamma_k\alpha_k^\dagger\alpha_k\right), \tag{4.7}$$

where

$$\gamma_k = \sum_{n=0}^{\infty}\lambda_n^+\varepsilon_h(k)\cos(kn) - 2J\lambda_n^-\sin[k(n+1)]. \tag{4.8}$$

This establishes the fact that the GGE density matrix can be constructed either from the local conservation laws (3.6), or from the mode occupation numbers n_k. This relationship generalizes to interacting integrable models, where the appropriate GGE can be formulated either in terms of the local integrals of motion generated from the transfer matrix, or from the mode occupation numbers $n_a(k) = Z_a^\dagger(k)Z_a(k)$, where $Z_a(k)$ are Faddeev-Zamolodchikov operators.[56,57]

V. TRUNCATED GENERALIZED GIBBS ENSEMBLES

In order to assess the importance of the various conserved quantities, it is useful to define ensembles that interpolate between the Gibbs distribution and the GGE. We define particular such truncated GGEs as follows. Given that the densities of the conservation laws $I_n^\pm$ involve $n+2$ neighboring sites, it is natural to retain only the "most local" conservation laws, i.e.,

$$\rho_{\rm tGGE}^{(y)} = \frac{1}{\mathcal{Z}_y}\exp\left(-\sum_{n=0}^{y-1}\sum_{\sigma=\pm}\left[\lambda_{n,y}^\sigma I_n^\sigma\right]\right). \tag{5.1}$$

Here y is an integer and $y = 1$ ($y = \infty$) corresponds to the Gibbs ensemble (GGE). The Lagrange multipliers $\lambda_{n,y}^\sigma$ are obtained from the requirements

$$\mathrm{Tr}\left[\left(I_n^\sigma\right)_{j,\dots,j+n+1}\rho_{\rm tGGE}^{(y)}\right] = \langle\Psi_0|\left(I_n^\sigma\right)_{j,\dots,j+n+1}|\Psi_0\rangle, \tag{5.2}$$

where $0 \leqslant n < y$. Equation (5.2) is a consequence of $[I_n^\sigma, H] = 0$ and the assumption that the stationary state after the quench is described by RDMs based on (5.1). For transverse-field quenches we have $\lambda^-_{n,y} = 0$, but the other Lagrange multipliers are different from their respective values in the full GGE, i.e.,

$$\lambda^+_{n,y} \neq \lambda^+_n . \tag{5.3}$$

We note that the correlation matrix of $\rho^{(y)}$ can be computed efficiently using FFT algorithms. This is in contrast to the case of theories with nontrivial scattering matrices, for which it is extremely difficult to reconstruct the Lagrange multipliers from the conservation laws.[58]

VI. DEFECTIVE GENERALIZED GIBBS ENSEMBLES

It is instructive to consider a second type of truncated GGE, where we retain an infinite, but incomplete set of integrals of motion. Such "defective" GGEs will allow us to ascertain the role of a particular local conservation law. We define the truncated defective GGE as the density matrix ($q < y$)

$$\rho^{(+q),y}_{\mathrm{tdGGE}} = \frac{1}{\mathcal{Z}_{(+q),y}} \exp\left(- \sum_{\substack{n=0 \\ n\neq q}}^{y} \left[\lambda^+_{n,(+q),y} I^+_n \right] \right), \tag{6.1}$$

in which the Lagrange multipliers $\lambda^+_{n,(+q)}$ are fixed by the system (4.2) with $n \leqslant y$, $n \neq q$, and we have used that the Lagrange multipliers $\lambda^-_{n,(+q),y}$ must vanish as a consequence of reflection symmetry around the origin. We then define the defective GGE as the limit $y \to \infty$ of truncated defective GGEs:

$$\rho^{(+q)}_{\mathrm{dGGE}} = \lim_{y\to\infty} \rho^{(+q),y}_{\mathrm{tdGGE}} . \tag{6.2}$$

In order to solve the system of equations (4.2) for the defective GGE it is useful to work in the mode occupation number representation (4.7), which reads as

$$\rho^{(+q)}_{\mathrm{dGGE}} = \frac{1}{\mathcal{Z}_{(+q)}} \exp\left(- \int_{-\pi}^{\pi} \frac{dk}{2\pi} \gamma^{(+q)}_k \alpha^\dagger_k \alpha_k \right), \tag{6.3}$$

where the Lagrange multipliers $\gamma^{(+q)}_k$ are subject to the set of equations

$$\begin{aligned} \int_{-\pi}^{\pi} \frac{dk}{2\pi} \left[\tanh\left(\frac{\gamma^{(+q)}_k}{2} \right) - \cos\Delta_k \right] \varepsilon(k) \cos(nk) = 0, \\ \int_{-\pi}^{\pi} \frac{dk}{2\pi} \left[\tanh\left(\frac{\gamma^{(+q)}_k}{2} \right) - \cos\Delta_k \right] \sin[(n+1)k] = 0. \end{aligned} \tag{6.4}$$

Guided by the fact that $\cos(nk)$ and $\sin[(n+1)k]$ form an orthonormal set of functions on $[-\pi,\pi]$, we look for a solution of the form

$$\tanh\left(\frac{\gamma^{(+q)}_k}{2} \right) = \cos\Delta_k - \kappa^+_q \frac{\cos(qk)}{\varepsilon(k)} , \tag{6.5}$$

where κ^+_q is a yet to be determined constant. We note that the value of κ^+_q affects the expectation values of local operators. For some cases κ^+_q can be easily determined as follows. Given that $|\tanh(x)| \leqslant 1$, (6.5) implies that

$$\left| \cos\Delta_k - \kappa^+_q \frac{\cos(qk)}{\varepsilon(k)} \right| \leqslant 1, \qquad \forall k. \tag{6.6}$$

Setting $k = 0,\pi$ then gives

$$\begin{aligned} |2J(h-1)\mathrm{sgn}(h_0-1) - \kappa^+_q| &\leqslant 2J|h-1|, \\ |2J(h+1) - (-1)^q \kappa^+_q| &\leqslant 2J(h+1) . \end{aligned} \tag{6.7}$$

Equations (6.7) allow us to identify cases, in which $\kappa^+_q = 0$:

(1) odd q and quenches within the same phase;
(2) even q and quenches across the critical point.

Importantly, $\kappa^+_q = 0$ implies that $\rho^{(+q)}_{\mathrm{dGGE}} \equiv \rho_{\mathrm{GGE}}$, i.e., the defective GGE is identical to the full GGE. This "GGE reconstruction" is a peculiarity of free-fermion models and can be traced back to the existence of conservation laws independent of the quench parameter (see also Ref. 59).

For general quenches and values of q, κ^+_q is determined by Eq. (6.2). We find that it takes the value corresponding to the maximal entanglement entropy (as shown in Fig. 9), although the entanglement entropy may be nonstationary under a variation of the excluded integral of motion (see Appendix D for further details).

VII. REDUCED DENSITY MATRICES IN THE TRANSVERSE-FIELD ISING CHAIN

In this section we summarize some basic features of RDMs in the TFIC. We note that most of the following discussion generalizes straightforwardly to other spin chains with free fermionic spectra such as the quantum XY model. Our starting point is a density matrix ρ describing the entire system, which we take to be of size L with periodic boundary conditions. We are interested in the limit $L \to \infty$, but it is convenient to start with a large, finite chain. The RDM of a subsystem consisting of ℓ spins $\frac{1}{2}$ at sites x_i, $i = 1,\ldots,\ell$, can be expressed in the form

$$\rho_{\{x_1,\ldots,x_\ell\}} = \frac{1}{2^\ell} \sum_{\{\alpha\}_\ell} \mathrm{Tr}\left[\rho\, \sigma^{\alpha_1}_{x_1} \ldots \sigma^{\alpha_\ell}_{x_\ell} \right] \sigma^{\alpha_1}_{x_1} \ldots \sigma^{\alpha_\ell}_{x_\ell} , \tag{7.1}$$

where $\alpha_i = 0,x,y,z$ and $\sigma^0 \equiv \mathrm{I}$. The quantum spins are mapped to (real) Majorana fermions by the Jordan-Wigner transformation (2.2). The nonlocality of the transformation (2.2) has important consequences for RDMs. First and foremost, if the spins are not adjacent, the map from spin to fermionic degrees of freedom does not have a simple reduction to the subspace of the Hilbert space formed by sites $\{x_1,\ldots,x_\ell\}$ because of Jordan-Wigner strings stretching between sites.[60,61] However, the RDM of a block of adjacent spins can be mapped one-to-one on a block of adjacent fermions,[62] provided that the first site of the block coincides with site 1, i.e., the origin of Jordan-Wigner strings. Then (7.1) can be represented in the form

$$\rho_\ell = \frac{1}{2^\ell} \sum_{\{\mu\}} \mathrm{Tr}\left[\rho\, a^{\mu_1}_1 \ldots a^{\mu_{2\ell}}_{2\ell} \right] a^{\mu_{2\ell}}_{2\ell} \ldots a^{\mu_1}_1 \tag{7.2}$$

with $\mu_j = 0,1$. An important quantity in what follows is the *correlation matrix* Γ,

$$\Gamma_{ij} = \mathrm{Tr}[\rho\, a_j a_i] - \delta_{ij}\,, \quad 1 \leqslant i,j \leqslant 2\ell. \tag{7.3}$$

In the cases of interest to us, the correlation matrix is of block-Toeplitz form

$$\Gamma = \begin{bmatrix} \Gamma_0 & \Gamma_{-1} & \dots & \Gamma_{1-\ell} \\ \Gamma_1 & \Gamma_0 & & \vdots \\ \vdots & & \ddots & \vdots \\ \Gamma_{\ell-1} & \dots & \dots & \Gamma_0 \end{bmatrix}, \tag{7.4}$$

where

$$\Gamma_l = \int_{-\pi}^{\pi} \frac{dk}{2\pi} e^{-ilk} \begin{pmatrix} -f(k) & g(k) \\ -g(-k) & f(k) \end{pmatrix}. \tag{7.5}$$

The TFIC Hamiltonian exhibits a $\mathbb{Z}_2$ symmetry

$$a_j \longrightarrow -a_j\,. \tag{7.6}$$

If the density ρ is invariant under the transformation (7.6) we have $\mathrm{Tr}[\rho\, a_j] = 0$, and as Wick's theorem applies to the Jordan-Wigner fermions we can express (7.2) as a Gaussian[62]

$$\rho_\ell = \frac{1}{Z} e^{\frac{1}{4}\sum_{mn} a_m W_{mn} a_n}\,, \tag{7.7}$$

where Z ensures that $\mathrm{Tr}\rho_\ell = 1$ and W is a skew symmetric $2\ell \times 2\ell$ Hermitian matrix related to Γ by

$$\tanh\frac{W}{2} = \Gamma. \tag{7.8}$$

We now turn to the three particular cases of interest, namely, those where ρ in (7.1) is a thermal density matrix, a GGE density matrix, or the density matrix after a global quantum quench of the transverse field in the TFIC.

A. Thermal density matrix

On a very large ring, the Hamiltonian has a block-diagonal structure (see Sec. II). The thermal density matrix is a function of the Hamiltonian and therefore inherits the same block structure

$$\rho_\beta = \left[\frac{1+e^{i\pi\mathcal{N}}}{2}\frac{e^{-\beta H_{\mathrm{R}}}}{Z_{\mathrm{R}}} + \frac{1-e^{i\pi\mathcal{N}}}{2}\frac{e^{-\beta H_{\mathrm{NS}}}}{Z_{\mathrm{NS}}}\right]. \tag{7.9}$$

It follows from this that only even operators have nonvanishing expectation values, i.e.,

$$\mathrm{Tr}(\rho_\beta \mathcal{O}) \neq 0 \to [e^{i\pi\mathcal{N}}, \mathcal{O}] = 0. \tag{7.10}$$

In the thermodynamic limit the difference between expectation values of local operators with respect to the R and NS sectors tends to zero, so that we may work exclusively in, e.g., the R sector. The resulting RDM of a contiguous block of spins is then Gaussian (7.7), (7.8) with

$$(\Gamma_\beta)_{ij} = \mathrm{Tr}\left[\frac{e^{-\beta H_R}}{Z_R} a_j a_i\right] - \delta_{ij}. \tag{7.11}$$

It can be written in the form (7.4) with

$$f(k) = 0\,, \quad g(k) = -ie^{i\theta_k}\tanh\left(\frac{\beta\varepsilon_h(k)}{2}\right). \tag{7.12}$$

B. GGE density matrix

It was shown in Ref. 32 (see also Refs. 24 and 31) that the RDM of the generalized Gibbs ensemble (4.1), (4.7) is Gaussian and can be expressed in the form (7.7), (7.8). The correlation matrix is given by

$$(\Gamma_{\mathrm{GGE}})_{ij} = \frac{1}{\mathcal{Z}}\mathrm{Tr}\big[e^{-\sum_{i,\sigma}\lambda_j^\sigma I_j^\sigma} a_j a_i\big] - \delta_{ij}. \tag{7.13}$$

It can be written in the form (7.4) with

$$f(k) = 0\,, \quad g(k) = -ie^{i\theta_k}\tanh\left(\frac{\gamma_k}{2}\right). \tag{7.14}$$

Here the γ_k's are related to the λ_m^σ's by (4.8) and the Bogoliubov angle θ_k is given in (2.6).

C. Truncated GGE density matrix

The correlation matrix of the truncated GGE defined in Sec. V is given by

$$\big(\Gamma^{(y)}_{\mathrm{tGGE}}\big)_{ij} = \frac{1}{\mathcal{Z}_y}\mathrm{Tr}\left[\exp\left(-\sum_{n=0}^{y-1}\sum_{\sigma=\pm}\big[\lambda^\sigma_{n,y} I^\sigma_n\big]\right) a_j a_i\right] - \delta_{ij}\,. \tag{7.15}$$

It can be written in the form (7.4) with

$$f(k) = 0\,, \quad g(k) = -ie^{i\theta_k}\tanh(P_{y-1}[\cos(k)]\varepsilon(k))\,. \tag{7.16}$$

Here $P_{y-1}(x)$ is a polynomial of order $y-1$, which is computed numerically.

D. Defective GGE density matrix

In Sec. VI we defined the defective GGE $\rho^{(q)}_{\mathrm{dGGE}}$ as the ensemble that lacks in the conservation law I_q^+. Its correlation matrix is given by

$$\big[\bar\Gamma^{(+q)}_{\mathrm{dGGE}}\big]_{ij} = \frac{1}{\mathcal{Z}^{(\mathrm{d})}_q}\mathrm{Tr}\left[\exp\left(-\sum_{\substack{n=0\\ n\neq q}}^{\infty}\lambda^+_{n,(+q)} I^+_n\right) a_j a_i\right] - \delta_{ij}\,. \tag{7.17}$$

It can be written in the form (7.4) with $f(k) = 0$ and [cf. Eq. (7.14)]

$$g(k) = -ie^{i\theta_k}\left[\tanh\left(\frac{\gamma_k}{2}\right) - \kappa_q^+\frac{\cos(qk)}{\varepsilon(k)}\right], \tag{7.18}$$

where κ_q^+ is computed numerically maximizing the entanglement entropy, which selects $\lambda^+_{q,(+q)} = 0$ whenever it is allowed. We note that the Fourier transform of Eq. (7.18), which is required to compute the correlation matrix (7.5), can be easily expressed in terms of the GGE correlators; for $|\ell| < q$ we have

$$\int_{-\pi}^{\pi}\frac{dk}{2\pi}e^{-i\ell k}g(k) = \int_{-\pi}^{\pi}\frac{dk}{2\pi}e^{-i\ell k}g_{\mathrm{GGE}}(k) + \frac{i\kappa_q}{4J}\mathrm{sgn}(\ln h)h^{\ell-1}e^{-|\ln h|q}\,. \tag{7.19}$$

Since κ_q^+ is a bounded function of q [cf. Eq. (6.7)], at fixed ℓ the fermionic correlators approach the GGE ones at least exponentially fast in q.

E. Quench density matrix

At zero temperature the ground state phase diagram of the TFIC exhibits ferromagnetic ($h < 1$) and paramagnetic ($h > 1$) phases, separated by a quantum critical point. In the ferromagnetic phase, the $\mathbb{Z}_2$ symmetry of the Hamiltonian is broken spontaneously. As we will see, this symmetry breaking has important effects on the time evolution of the density matrix.

1. *Quenches originating in the paramagnetic phase*

Here, at $t > 0$ the full quench density matrix is

$$\rho(t) = |\Psi_t\rangle\,\langle\Psi_t|, \tag{7.20}$$

where the state $|\Psi_t\rangle$ is given in (2.13). As a result of the squeezed-state form of $|\Psi_t\rangle$, Wick's theorem applies to averages calculated with respect to $\rho(t)$, and RDMs are Gaussians of the form (7.7), (7.8), with correlation matrix

$$\Gamma(t) = {}_{\rm NS}\langle 0|e^{iH_{\rm NS}t}a_j a_i e^{-iH_{\rm NS}t}|0\rangle_{\rm NS} - \delta_{ij}\,. \tag{7.21}$$

This is of the form (7.4) with

$$\begin{aligned} g(k) &= -ie^{i\theta_k}[\cos\Delta_k - i\sin\Delta_k\cos(2\varepsilon_h(k)t)],\\ f(k) &= \sin\Delta_k\sin(2\varepsilon_h(k)t), \end{aligned} \tag{7.22}$$

where $e^{i\theta_k}$ is given by (2.6).

2. *Quenches originating in the ferromagnetic phase*

Given the initial state (2.14), the post-quench density matrix of the full system is

$$\begin{aligned} \rho(t) &= |\Psi_t\rangle\langle\Psi_t|,\\ |\Psi_t\rangle &= \frac{e^{-iH_{\rm R}t}|0;h_0\rangle_{\rm R} + e^{-iH_{\rm NS}t}|0;h_0\rangle_{\rm NS}}{\sqrt{2}}. \end{aligned} \tag{7.23}$$

Importantly, RDMs are no longer Gaussian in this case. We will discuss how to cope with this complication in Sec. XI. It is known[32] that in the stationary state RDMs are Gaussian with a correlation matrix equal to the $t \to \infty$ limit of (7.21).

VIII. DISTANCES ON THE SPACE OF RDMS

In the following, we focus on RDMs for finite subsystems of lattice models with a finite dimensional Hilbert space at each site. In this case the RDMs are finite dimensional matrices, and a simple way to define a distance between two density matrices is by means of a matrix norm

$$d_a(\rho,\rho') = \|\rho - \rho'\|_a\,. \tag{8.1}$$

Here the index a labels different matrix norms. As we are dealing with finite matrices, all norms are equivalent in the sense that

$$c_{ab}\|\rho\|_a \leqslant \|\rho\|_b \leqslant c_{ba}^{-1}\|\rho\|_a\,, \tag{8.2}$$

where c_{ab} and c_{ba} are positive numbers that depend on the matrix dimension but are independent of ρ. One consequence of (8.2) is that if the distance between two matrices approaches zero when some external parameter p is tuned to a value $\bar{p}$, the dependence of the distance on $p - \bar{p}$ is almost independent of the norm. On the other hand, the dependence on matrix dimension is in general very different for different norms. This is important for our purposes because the matrix dimension is related to the size of the subsystem under consideration, and it is principally desirable to be able to compare distances between different sizes.

From a technical point of view, the distance induced by the Frobenius norm[63]

$$\|A\|_F \equiv \sqrt{{\rm Tr}[A^\dagger A]} \tag{8.3}$$

is generally the easiest to calculate. On the other hand, it has the drawback that the physical interpretation of the distance is less transparent than for some other norms. For instance, given two density matrices ρ and ρ', a very natural question is how different expectation values of local observables are in the two ensembles. We now discuss this question for the particular case of spin-$\frac{1}{2}$ quantum spin chains. Here the most important local observables are products of Pauli matrices. These are particular cases of involutions $\hat{O}^2 = {\rm I}$, for which the following inequality holds:

$$|{\rm Tr}[(\rho - \rho')\hat{O}]| \leqslant \|\rho - \rho'\|_1\,. \tag{8.4}$$

Here

$$\|A\|_1 \equiv {\rm Tr}[\sqrt{AA^\dagger}] \tag{8.5}$$

is the trace norm. From Eq. (8.4) it is evident that the trace distance provides an upper bound for the difference between the expectation values of observables in the two states: if $\|\rho - \rho'\|_1 < \epsilon$, then the expectation values of all (local) observables will agree in the two ensembles within accuracy ϵ. In terms of the Frobenius distance we have instead (here we use that the local Hilbert space is two dimensional)

$$|{\rm Tr}[(\rho - \rho')\hat{O}]| \leqslant \|\rho - \rho'\|_1 \leqslant 2^{\ell/2}\|\rho - \rho'\|_F\,. \tag{8.6}$$

On the other hand, we have

$$|{\rm Tr}[(\rho - \rho')\hat{O}]| \leqslant |{\rm Tr}[\rho\hat{O}]| + |{\rm Tr}[\rho'\hat{O}]| \leqslant 2, \tag{8.7}$$

where in the last step we have used that for involutions $\hat{O}$

$$|{\rm Tr}[\rho\hat{O}]| \leqslant \sum_j |\,(\rho)_{jj}\,| = {\rm tr}\sqrt{\rho^\dagger\rho} = 1. \tag{8.8}$$

Combining (8.7) and (8.6) we see that as long as $\|\rho - \rho'\|_F \gtrsim 2^{1-\ell/2}$, the Frobenius distance does not provide useful information about expectation values. It is shown in Appendix A that for sufficiently large ℓ this is always the case.

A second problem with using the Frobenius norm as a distance is that the norms of RDMs at late times after a quantum quench, as well as the norms of RDMs describing Gibbs or generalized Gibbs ensembles, generally are exponentially small in the subsystem size. Given the upper bound derived in Appendix A

$$\|\rho - \rho'\|_F \leqslant \sqrt{\|\rho\|_F^2 + \|\rho'\|_F^2}, \tag{8.9}$$

this implies that in these cases of interest $\|\rho - \rho'\|_F$ is exponentially small in subsystem size. This shows that the Frobenius norm itself is not a convenient measure for the distance between two density matrices. The same problem occurs for the operator norm $\|A\|_{\rm op} = \sqrt{\lambda_{\rm max}}$, where $\lambda_{\rm max}$ is the largest eigenvalue of $A^\dagger A$. This norm was used for example in Ref. 20 to analyze the relaxation properties of

small subsystems after a quench into a nonintegrable model. Indeed we have

$$\|\rho - \rho'\|_{op} \leqslant \|\rho\|_{op} + \|\rho'\|_{op}\,, \tag{8.10}$$

and the maximal eigenvalues of RDMs for large subsystems are generally exponentially small in subsystem size.

A. Definition of the distance

In order to circumvent the problem described above, we define our "distance"[64] on the space of RDMs as

$$\mathcal{D}(\rho,\rho') \equiv \frac{\|\rho - \rho'\|_F}{\sqrt{\|\rho\|_F^2 + \|\rho'\|_F^2}}\,. \tag{8.11}$$

An upper bound. Using the upper bound derived in (A1), we see that

$$\mathcal{D}(\rho,\rho') \leqslant 1. \tag{8.12}$$

A lower bound. A lower bound for $\mathcal{D}(\rho,\rho')$ can be established by means of the triangle inequality $\|\rho - \rho'\|_F \geqslant |\,\|\rho\|_F - \|\rho'\|_F\,|$. Using that the Frobenius norm of a RDM is related to the second Rényi entropy by

$$S_2 \equiv -\ln \mathrm{Tr}[\rho^2] = -\ln \|\rho\|_F^2, \tag{8.13}$$

we find that

$$\|\rho - \rho'\| \geqslant \left|\exp\left(-\frac{S_2}{2}\right) - \exp\left(-\frac{S_2'}{2}\right)\right|. \tag{8.14}$$

This provides the desired lower bound

$$\mathcal{D}(\rho,\rho') \geqslant \frac{|e^{-S_2/2} - e^{-S_2'/2}|}{\sqrt{e^{-S_2} + e^{-S_2'}}}\,. \tag{8.15}$$

We note that the bound (8.15) is independent of subsystem size ℓ as long as the second Rényi entropies of the two ensembles differ at least by a constant (when viewed as functions of ℓ).

B. Distance between two thermal ensembles

In order to establish a benchmark for (8.11), it is useful to consider the distance between the RDMs of two thermal ensembles at slightly different inverse temperatures β and β' (but the same Hamiltonian). Then

$$\mathcal{D}(\rho_\beta,\rho_{\beta'}) \approx \frac{\left\|\frac{\partial\rho_\beta}{\partial\beta}\right\|_F}{\|\rho_\beta\|_F}\,\frac{1}{\sqrt{2}}|\beta - \beta'|. \tag{8.16}$$

For a sufficiently large subsystem (and a local Hamiltonian), the first factor on the right-hand side can be expressed as

$$\frac{\left\|\frac{\partial\rho_\beta}{\partial\beta}\right\|_F^2}{\|\rho_\beta\|_F^2} = \frac{\|\rho_\beta(\langle H\rangle_\beta - H)\|_F^2}{||\rho_\beta||_F^2} = \frac{\mathrm{Tr}\left[\rho_\beta^2(\langle H\rangle_\beta - H)^2\right]}{\mathrm{Tr}\rho_\beta^2}$$
$$= \langle(\langle H\rangle_\beta - H)^2\rangle_{2\beta}, \tag{8.17}$$

where $\langle\mathcal{O}\rangle_\beta = \mathrm{Tr}(\rho_\beta\mathcal{O})$. For a large subsystem, this is proportional to the square of its size, and hence

$$\frac{\left\|\frac{\partial\rho_\beta}{\partial\beta}\right\|_F}{\|\rho_\beta\|_F} \propto \ell. \tag{8.18}$$

We conclude that the distance between two thermal RDMs on a subsystem of size ℓ and $\beta \approx \beta'$ is

$$\mathcal{D}(\rho_\beta,\rho_{\beta'}) \propto \ell|\beta - \beta'|. \tag{8.19}$$

As expected, this is proportional to the difference in temperatures, but there is also a factor of ℓ. The latter is important if one is interested in comparing the distance between two ensembles for different subsystem sizes.

C. Distance between two GGEs

The above discussion carries over to the case of two generalized Gibbs ensembles (4.1), with slightly different values of Lagrange multipliers λ_m^σ. The leading contribution to the distance is given by

$$\mathcal{D}(\rho_{\mathrm{GGE}},\rho'_{\mathrm{GGE}}) \approx \sum_{m,\sigma} \frac{\left\|\frac{\partial\rho_{\mathrm{GGE}}}{\partial\lambda_m^\sigma}\right\|_F}{||\rho_{\mathrm{GGE}}||_F}\,\frac{1}{\sqrt{2}}|\lambda_m^\sigma - \lambda'^\sigma_m|. \tag{8.20}$$

A calculation similar to the thermal case shows that for large subsystem size

$$\frac{\left\|\frac{\partial\rho_{\mathrm{GGE}}}{\partial\lambda_m^\sigma}\right\|_F}{||\rho_{\mathrm{GGE}}||_F} \propto \ell. \tag{8.21}$$

D. Information on observables contained in the distance

Let us consider the situation where the distance between two reduced density matrices ρ_1 and ρ_2 defined on an interval of length ℓ becomes small, and denote the corresponding averages of local operators on said interval by

$$\langle\mathcal{O}\rangle_a = \mathrm{Tr}[\rho_a\mathcal{O}], \quad a = 1,2. \tag{8.22}$$

By expanding the density matrices in a complete basis of Hermitian involutions we can show that

$$\mathcal{D}(\rho_1,\rho_2) = \sqrt{\frac{\sum_{\mathcal{O}}(\langle\mathcal{O}\rangle_2 - \langle\mathcal{O}\rangle_1)^2}{\sum_{\mathcal{O}}\left(\langle\mathcal{O}\rangle_2^2 + \langle\mathcal{O}\rangle_1^2\right)}}. \tag{8.23}$$

Defining an average

$$\overline{f(\mathcal{O})} \equiv \sum_{\mathcal{O}} P(\mathcal{O})f(\mathcal{O}), \quad P(\mathcal{O}) = \frac{\langle\mathcal{O}\rangle_1^2 + \langle\mathcal{O}\rangle_2^2}{\sum_{\mathcal{Q}}\langle\mathcal{Q}\rangle_1^2 + \langle\mathcal{Q}\rangle_2^2}, \tag{8.24}$$

we can express the distance (8.11) as

$$\mathcal{D}(\rho_1,\rho_2) = (\overline{[R(\mathcal{O})]^2})^{1/2}. \tag{8.25}$$

Here,

$$R(\mathcal{O}) \equiv \frac{|\,\langle\mathcal{O}\rangle_1 - \langle\mathcal{O}\rangle_2\,|}{\sqrt{\langle\mathcal{O}\rangle_1^2 + \langle\mathcal{O}\rangle_2^2}} \tag{8.26}$$

is the relative difference between the ensembles described by ρ_1 and ρ_2, respectively. This implies that $\mathcal{D}(\rho_1,\rho_2)$ measures the mean relative difference of the expectation values of all local operators, averaged with respect to the probability distribution (8.24).

E. Distance between two Gaussian density matrices

The distance (8.11) between two Gaussian RDMs $\rho[\Gamma]$ and $\rho[\Gamma']$ can be expressed in terms of their correlation matrices following Ref. 60. Given the definition of the distance

$$\mathcal{D}(\rho,\rho') = \frac{\sqrt{\mathrm{Tr}(\rho^2+\rho'^2-2\rho\rho')}}{\sqrt{\mathrm{Tr}(\rho^2)+\mathrm{Tr}(\rho'^2)}}, \tag{8.27}$$

we require tractable expressions for the quantities

$$\mathrm{Tr}(\rho[\Gamma]\rho[\Gamma']). \tag{8.28}$$

This is achieved in two steps. First, we note that the product of two Gaussian RDMs (7.7) is itself Gaussian:[60]

$$\exp\left(\frac{1}{4}\sum_{i,j} W_{ij}a_i a_j\right)\exp\left(\frac{1}{4}\sum_{i,j}\widetilde{W}_{ij}a_i a_j\right) = \exp\left(\frac{1}{4}\sum_{i,j}[\ln(e^W e^{\widetilde{W}})]_{ij}a_i a_j\right). \tag{8.29}$$

This can be seen by expanding the left-hand side of (8.29) by means of the Baker-Campbell-Hausdorff formula in terms of multiple commutators, and then observing that the commutator of quadratic operators is quadratic and gives rise to a commutator between the matrices W that characterize the 2-forms

$$\left[\frac{1}{4}\sum_{i,j} W_{ij}a_i a_j, \frac{1}{4}\sum_{i,j}\widetilde{W}_{ij}a_i a_j\right] = \frac{1}{4}\sum_{i,j}[[W,\widetilde{W}]]_{ij}a_i a_j\,. \tag{8.30}$$

Second, using results for the second Rényi entropy,[65] one can relate the Frobenius norm of a Gaussian RDM to the correlation matrix by

$$\mathrm{Tr}[\rho[\Gamma]^2] = \left(\det\left|\frac{\mathrm{I}+\Gamma^2}{2}\right|\right)^{\frac{1}{2}}. \tag{8.31}$$

Combining (8.31) and (8.29), one can then show[60] that

$$\{\Gamma,\tilde{\Gamma}\} \equiv \mathrm{Tr}[\rho[\Gamma]\rho[\tilde{\Gamma}]] = \left(\det\left|\frac{\mathrm{I}+\Gamma\tilde{\Gamma}}{2}\right|\right)^{\frac{1}{2}}. \tag{8.32}$$

Here, we have used that $\mathrm{Tr}\,[\rho_1\rho_2] \geqslant 0$, which is a consequence of density matrices being positive semidefinite operators. Finally, substituting (8.32) into (8.27), we obtain the following result for the distance between two Gaussian RDMs:

$$\mathcal{D}(\rho[\Gamma],\rho[\tilde{\Gamma}]) = \left[1-\frac{2\{\Gamma,\tilde{\Gamma}\}}{\{\Gamma,\Gamma\}+\{\tilde{\Gamma},\tilde{\Gamma}\}}\right]^{\frac{1}{2}}. \tag{8.33}$$

Given that the correlation matrices are only 2ℓ dimensional (with ℓ the subsystem size), (8.33) provides a very efficient way of computing distances for large subsystem sizes.

IX. SINGLE-SITE SUBSYSTEM

It is instructive to consider the time evolution of the RDM describing a single-site subsystem in some detail. In this case, the RDM of site 1 can be expressed in the form

$$\rho_1(t) = \frac{\mathrm{I}}{2} + \vec{m}(t)\cdot\vec{\sigma}_1\,, \tag{9.1}$$

where $\vec{m}(t)$ is the magnetization per site at time t after the quench, i.e.,

$$m^\alpha(t) = \tfrac{1}{2}\langle\Psi_t|\sigma_1^\alpha|\Psi_t\rangle. \tag{9.2}$$

The RDM of the generalized Gibbs ensemble describing the stationary state is

$$\rho_{\mathrm{GGE},1} = \frac{\mathrm{I}}{2} + m^z_{\mathrm{stat}}\sigma_1^z, \tag{9.3}$$

where

$$m^z_{\mathrm{stat}} = \int_{-\pi}^{\pi}\frac{dk}{4\pi}e^{i\theta_k}\cos\Delta_k. \tag{9.4}$$

Finally, the RDM of the thermal ensemble described by ρ_β, whose inverse temperature β is fixed by the requirement

$$\lim_{L\to\infty}\frac{1}{L}\langle\Psi_0|H(h)|\Psi_0\rangle = \lim_{L\to\infty}\frac{1}{L}\mathrm{Tr}[\rho_\beta H(h)], \tag{9.5}$$

is given by

$$\rho_{\beta,1} = \frac{\mathrm{I}}{2} + m^z_\beta\sigma_1^z\,. \tag{9.6}$$

Here the transverse magnetization per site is

$$m^z_\beta = \int_{-\pi}^{\pi}\frac{dk}{4\pi}e^{i\theta_k}\tanh\left(\frac{\beta\varepsilon_k}{2}\right). \tag{9.7}$$

A. Quenches originating in the paramagnetic phase

Here the $\mathbb{Z}_2$ symmetry enforces

$$m^x(t) = m^y(t) = 0. \tag{9.8}$$

The z component of the magnetization per site is

$$m^z(t) = \int_{-\pi}^{\pi}\frac{dk}{4\pi}e^{i\theta_k}[\cos\Delta_k - i\sin\Delta_k\cos(2\varepsilon_k t)]. \tag{9.9}$$

For late times we may evaluate the integral by means of a stationary phase approximation, which gives

$$m^z(t) \simeq m^z_{stat} + \frac{c(t)}{(Jt)^{3/2}}, \tag{9.10}$$

where

$$c(t) = \frac{(h-h_0)\cos(4Jt|1-h|-\pi/4)}{8|h_0-1|\sqrt{\pi|h-1|}} + \frac{(h-h_0)\cos(4Jt|1+h|+\pi/4)}{8|h_0+1|\sqrt{\pi|h+1|}}. \tag{9.11}$$

The distance between $\rho_1(t)$ and the generalized Gibbs RDM at late times then decays to zero like a power law with exponent $\frac{3}{2}$:

$$\mathcal{D}(\rho_1(t),\rho_{\mathrm{GGE},1}) = \frac{\sqrt{2}|m^z(t)-m^z_{stat}|}{\sqrt{1+2[m^z(t)]^2+2\left(m^z_{\mathrm{GGE}}\right)^2}} \sim \sqrt{\frac{2c^2(t)}{1+4\left(m^z_{stat}\right)^2}}(Jt)^{-\frac{3}{2}}. \tag{9.12}$$

On the other hand, the distance between $\rho_1(t)$ and the thermal RDM approaches a constant at late times

$$\mathcal{D}(\rho_1(t),\rho_{\beta,1}) = \frac{\sqrt{2}|m^z(t)-m^z_\beta|}{\sqrt{1+2[m^z(t)]^2+2(m^z_\beta)^2}} \sim \frac{\sqrt{2}|m^z_{stat}-m^z_\beta|}{\sqrt{1+2(m^z_{stat})^2+2(m^z_\beta)^2}} + \mathcal{O}[(Jt)^{-\frac{3}{2}}]. \quad (9.13)$$

B. Quenches originating in the ferromagnetic phase

Here all three components of the magnetization per site are nonzero. The component along the transverse field direction is again given by (9.9), while the late-time asymptotics of $m^x(t)$ has been calculated in[31]

$$m^x(t) = \tfrac{1}{2}\sqrt{\mathcal{C}^x_{FF}}e^{t\int_0^\pi \frac{dk}{\pi}\ln\cos\Delta_k\varepsilon'_k}. \quad (9.14)$$

Here, $\mathcal{C}^x_{FF}$ is a known amplitude and $\varepsilon'_k = \frac{d\varepsilon_h(k)}{dk}$. Finally, the Heisenberg equation of motion for $\sigma^x_1(t)$ relates the y and x components:

$$m^y(t) = \frac{1}{2Jh}\frac{dm^x(t)}{dt}. \quad (9.15)$$

Importantly, $m^{x,y}(t)$ exhibit exponential decay in time. In contrast, $m^z(t)$ again decays like a power law with exponent $\frac{3}{2}$ and therefore will dominate the late-time behavior. Hence, at sufficiently late times, the distances of $\rho_1(t)$ to GGE and thermal RDMs are again given by (9.13) and (9.12), respectively. So, for a single-site subsystem the spontaneous symmetry breaking only modifies the intermediate time behavior of the distances. As we will see, this holds true also for larger subsystems.

X. LARGER SUBSYSTEMS FOR QUENCHES FROM THE PARAMAGNETIC PHASE

For quenches with $h_0 > 1$ and in the thermodynamic limit, we determine the distance between the quench RDM and that of an appropriate thermal or generalized Gibbs ensemble by means of relation (8.33). The correlation matrices for all cases are of the form (7.4), (7.5) with elements given in (7.12), (7.14), and (7.22), respectively. For a subsystem of size ℓ this requires the calculation of determinants of $2\ell\times 2\ell$ matrices, which is done numerically. Results for a quench from $h_0 = 1.2$ to $h = 3$ and subsystem sizes $\ell = 10,20,30,\ldots,150$ are shown in Figs. 2 and 3. We see that the distance between quench and Gibbs RDMs tends to a ℓ-dependent constant at late times. This establishes that subsystems do not thermalize. On the other hand, as can be seen from Fig. 3, at sufficiently late times the distance between $\rho_\ell(t)$ and $\rho_{\mathrm{GGE},\ell}$ decays to zero in a universal power-law fashion

$$\mathcal{D}(\rho_\ell(t),\rho_{\mathrm{GGE},\ell}) \overset{Jt\gg 1}{\to} k(\ell)(Jt)^{-3/2}+\cdots. \quad (10.1)$$

The quality of the fit (10.1) is shown in Fig. 4. The large-ℓ asymptotics of the function $k(\ell)$ can be inferred as follows. On surfaces with constant, small $\mathcal{D}$ the time scales as $t\sim\ell^{4/3}$ as

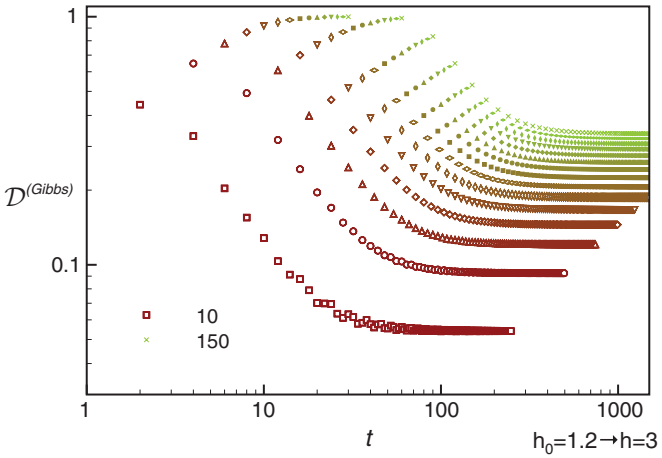

FIG. 2. (Color online) Normalized distance $\mathcal{D}^{\mathrm{Gibbs}} = \mathcal{D}(\rho_\ell(t),\rho^\beta_\ell)$ after a quench within the paramagnetic phase for subsystem sizes $\ell = 10,20,\ldots,150$. As ℓ increases, the color fades from brown to green, the symbols become smaller, and the curves narrower. At late times the distances tend to constants depending on subsystem size.

is shown in Fig. 5. This in turn implies that

$$k(\ell)\sim\ell^2. \quad (10.2)$$

A. Relaxation time

We may extract a relaxation time from the behavior of the distance by using the connection to averaged differences in the expectation values of local operators established in Sec. VIII D. The distance can be written as

$$\mathcal{D}(\rho_{\mathrm{GGE},\ell},\rho_\ell(t)) = (\overline{[R(\mathcal{O})]^2})^{1/2}, \quad (10.3)$$

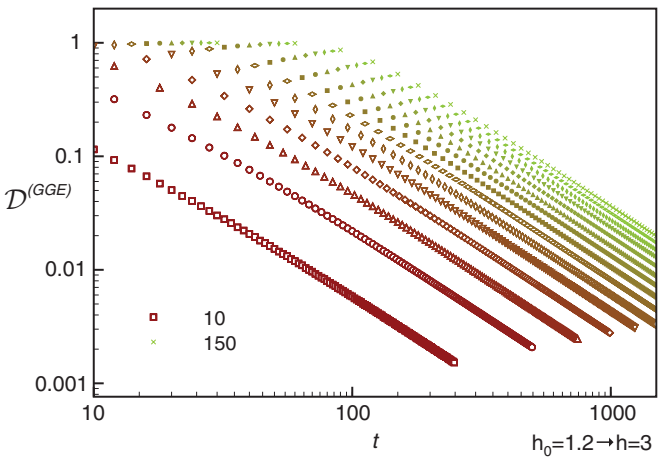

FIG. 3. (Color online) Normalized distance $\mathcal{D}^{\mathrm{GGE}} = \mathcal{D}(\rho_\ell(t),\rho^{\mathrm{GGE}}_\ell)$ after a quench within the paramagnetic phase for subsystem sizes $\ell = 10,20,\ldots,150$. As ℓ increases, the color fades from brown to green, the symbols become smaller, and the curves narrower. At late times, $D(\rho_\ell(t),\rho^{\mathrm{GGE}}_\ell)$ tends to zero in a universal power-law fashion $\propto (Jt)^{-3/2}$.

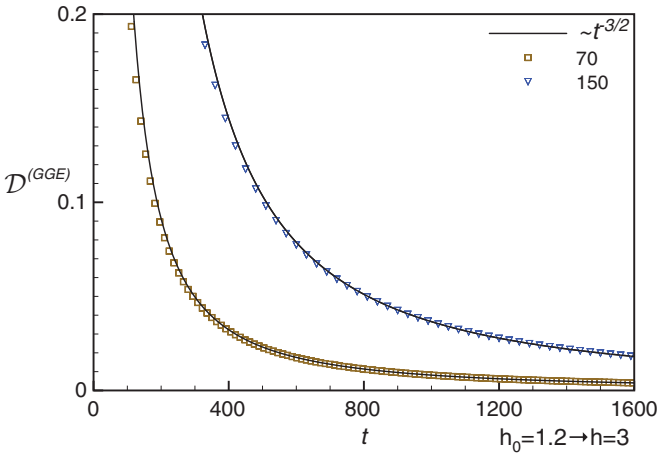

FIG. 4. (Color online) Distance $\mathcal{D}^{\rm GGE} = \mathcal{D}(\rho_\ell(t), \rho_\ell^{\rm GGE})$ after a quench within the paramagnetic phase for two representative values $\ell = 70, 150$. We used the same notations of Fig. 3. The black dashed curves are best fits to the form $\mathcal{D} = at^{-3/2}$.

where

$$R(\mathcal{O}) \equiv \frac{|\langle\mathcal{O}\rangle_t - \langle\mathcal{O}\rangle_{\rm GGE}|}{\sqrt{\langle\mathcal{O}\rangle_t^2 + \langle\mathcal{O}\rangle_{\rm GGE}^2}}, \tag{10.4}$$

and the bar denotes the average (8.24). Using that

$$\overline{R(\mathcal{O})} \leqslant \sqrt{\overline{[R(\mathcal{O})]^2}} = \mathcal{D}(\rho_{{\rm GGE},\ell}, \rho_\ell(t)), \tag{10.5}$$

and then substituting the asymptotic behavior (10.1), (10.2) into the right-hand side, we obtain

$$\overline{R(\mathcal{O})} \lesssim \ell^2 t^{-3/2}. \tag{10.6}$$

Bounding the right-hand side by a (small) constant, we obtain a time scale $t^*_{\rm rms}$ associated with the relaxation of the average relative error with respect to the distribution (8.24):

$$t^*_{\rm rms} \sim \ell^{4/3}. \tag{10.7}$$

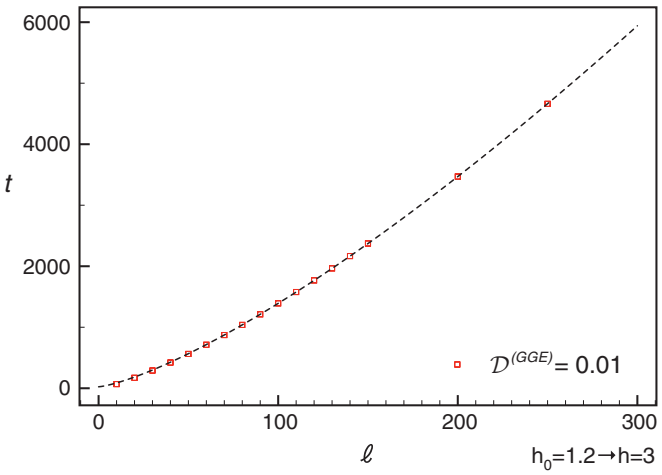

FIG. 5. (Color online) Dependence of time on subsystem size at fixed distance $\mathcal{D}(\rho_\ell(t), \rho_\ell^{\rm GGE}) = 0.01$ for the same parameters as in Fig. 3. The dashed curve is the best fit to the functional form $t = a + b\ell^{4/3}$.

It is not simple to identify the observables that give significant contribution to the average since it depends both on their "multiplicity" in the subsystem (produced by translational invariance and other symmetries) and on the expectation values. We note that the relaxation time $t^*_{\rm rms}$ is very different from the time scales identified in Ref. 32 in the time evolution of the two point functions of spin operators for quenches within the paramagnetic phase.

B. Distance from truncated generalized Gibbs ensembles

Having established that the distance between quench and GGE reduced density matrices tends to zero as a universal power law at late times, a natural question is how close the quench RDM is to the truncated GGEs (5.1), which retain only finite numbers of conservation laws.

A representative example for a quench within the paramagnetic phase is shown in Fig. 6. We see that at sufficiently late times, the distances converge to constant values. However, increasing the range (and number) of conservation laws, the values of these plateaux decrease, signaling that retaining more conservation laws gives better descriptions. In an intermediate time window, the extent of which grows with y, the distance decays in a universal $t^{-3/2}$ power-law fashion. In Fig. 7 we consider the distance

$$\mathcal{D}^{(y)}_\infty = \lim_{t\to\infty} \mathcal{D}\big(\rho_\ell(t), \rho^{(y)}_{{\rm tGGE},\ell}\big) = \mathcal{D}\big(\rho_{{\rm GGE},\ell}, \rho^{(y)}_{{\rm tGGE},\ell}\big) \tag{10.8}$$

between the RDMs of the truncated and full generalized Gibbs ensembles as a function of the parameter y. For a given subsystem size ℓ, this corresponds to plotting the values of the plateaux seen in Fig. 6 against the corresponding values of y. The distance is seen to start decaying exponentially as a function of y as soon as $y \gtrsim \ell$.

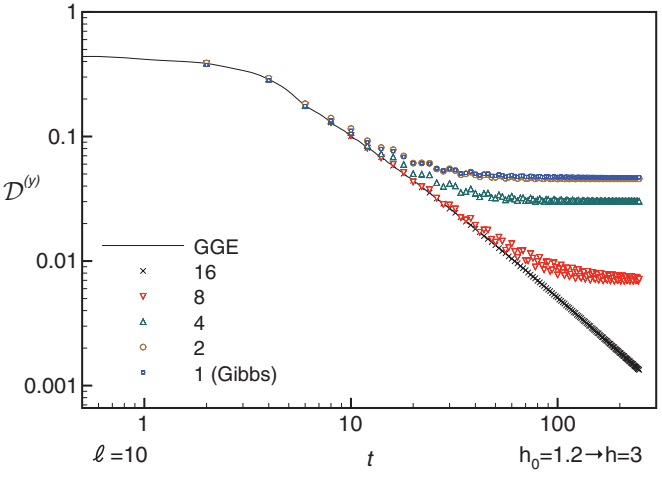

FIG. 6. (Color online) Distance $\mathcal{D}^{(y)} = \mathcal{D}(\rho_\ell(t), \rho^{(y)}_{{\rm tGGE},\ell})$ at fixed length $\ell = 10$ between quench and truncated GGE reduced density matrices for $y = 1,2,4,8,16$ and a quench within the paramagnetic phase. Here y is the maximal range of the densities of local conservation laws included in the definition of the ensemble. As the number of conservation laws is increased, the time window, in which the distance decays as $t^{-3/2}$, increases. At very late times all distances with finite y saturate to nonzero values.

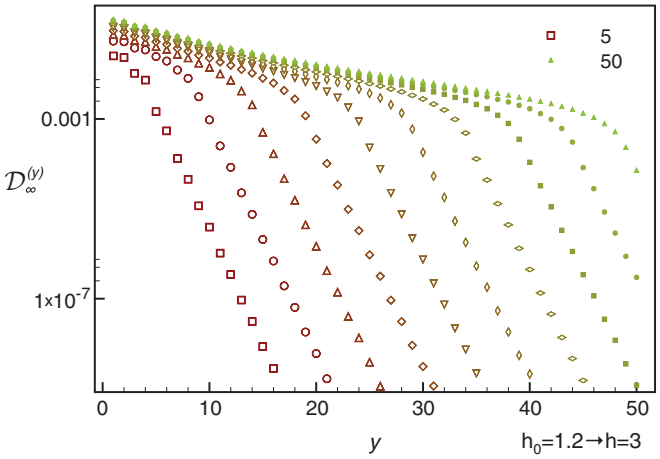

FIG. 7. (Color online) Distance $\mathcal{D}_\infty^{(y)} = \mathcal{D}(\rho_{\mathrm{GGE},\ell}, \rho_{\mathrm{tGGE},\ell}^{(y)})$ between the GGE and the truncated GGEs obtained by imposing local conservation laws with densities involving at most $y+1$ consecutive sites. The quench is from $h_0 = 1.2$ to $h = 3$ and the subsystem size ranges from $\ell = 5$ to 50. Colors and sizes change gradually as a function of the size ℓ. For $y > \ell$, the distance starts decaying exponentially in y, with an ℓ-independent decay constant.

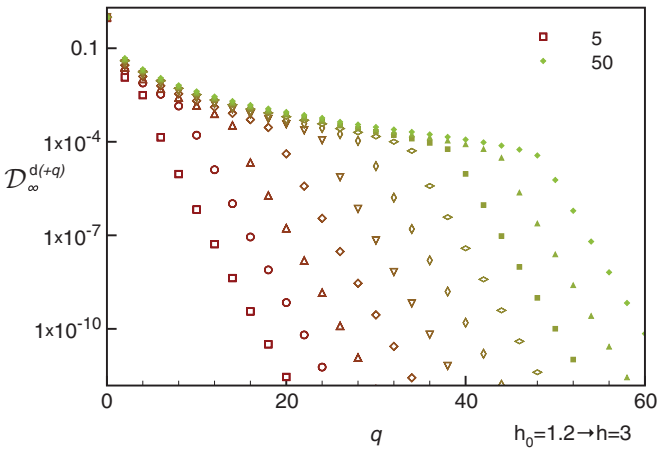

FIG. 8. (Color online) Distance $\mathcal{D}_\infty^{\mathrm{d}(+q)} = \mathcal{D}(\rho_{\mathrm{GGE},\ell}, \rho_{\mathrm{dGGE},\ell}^{(+q)})$ for a quench within the paramagnetic phase, for subsystem lengths $\ell = 5, 10, \ldots, 50$. The excluded conservation law is I_q^+ with even q. Colors and sizes change gradually as a function of the length. When $y > \ell$, the distance starts decaying exponentially with a decay length given by Eq. (10.10).

There are two main conclusions of the above analysis:

(1) Including more local conservation laws improves the description of the stationary state.

(2) The description of the stationary state improves rapidly, once the range $y+1$ of all conservation laws not included in the truncated GGE exceeds the subsystem size ℓ.

C. Distance from defective generalized Gibbs ensembles

We now turn to the role played by particular local conservation laws. We find that the distance between quench and defective GGE reduced density matrices for a given quench and subsystem size tends to a constant at late times, i.e.,

$$\lim_{t\to\infty} \mathcal{D}\big(\rho_\ell(t), \rho_{\mathrm{dGGE},\ell}^{(q)}\big) \equiv \mathcal{D}_\infty^{\mathrm{d}(+q)}. \tag{10.9}$$

The dependence of this asymptotic value on the subsystem size ℓ and the integer q is shown in Fig. 8 for a quench within the paramagnetic phase. We see that $\mathcal{D}_\infty^{\mathrm{d}(+q)}$ exhibits an exponential decay in q as soon as $q \gtrsim \ell$. This is similar to the behavior observed in the truncated GGE case. The decay length can be calculated from the large-q asymptotics of Eq. (7.19). By series expanding Eq. (8.33) to second order in $\Gamma_{\mathrm{dGGE}}^{(+q)} - \Gamma_{\mathrm{GGE}}$ we obtain

$$\mathcal{D}_\infty^{\mathrm{d}(+q)} \overset{y\gg\ell}{\sim} |\kappa_q^+| e^{-|\ln h|(q-\ell)}. \tag{10.10}$$

Numerically we find that $\kappa_q^+ \sim 1/q^2$.

1. *"GGE reconstruction"*

In Sec. VI we discussed the issue that, for certain quenches and omitted conservation laws I_q^+, the corresponding defective GGE is identical to the full generalized Gibbs ensemble. We now return to this point. In Fig. 9 we consider the truncated, defective GGE for a quench across the critical point from $h_0 = 2$ to $h = 0.5$ for a subsystem of length $\ell = 5$. We plot the distance between the reduced density matrices of the appropriate GGE and the truncated, defective GGE with y integrals of motion, where I_q^+ ($q < y$) has been excluded, i.e.,

$$\mathcal{D}_\infty^{\mathrm{d}(+q),y} = \mathcal{D}\big(\rho_{\mathrm{GGE},\ell}, \rho_{\mathrm{tdGGE},\ell}^{(+q),y}\big). \tag{10.11}$$

As discussed in Sec. VI, for even q we expect this distance to approach zero, when the number y of conservation laws goes to infinity. This behavior is clearly observed in Fig. 9. This implies that the corresponding conservation laws do not affect averages of local operators. As discussed before, this is a particular feature of free theories, where $H(h_0)$ and $H(h)$ generically share certain local conservation laws.

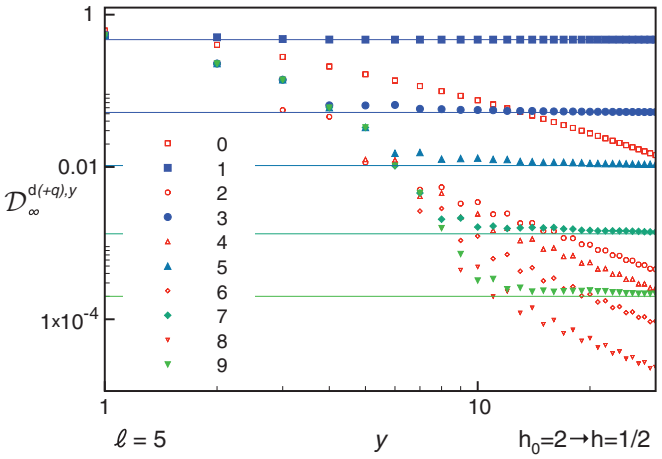

FIG. 9. (Color online) Distance $\mathcal{D}_\infty^{\mathrm{d}(+q),y} = \mathcal{D}(\rho_{\mathrm{GGE},\ell}, \rho_{\mathrm{dtGGE},\ell}^{(+q),y})$ for a quench across the critical point between the GGE and the defective truncated GGE RDMs for a subsystem of five consecutive spins, as a function of the number y of retained conservation laws. Each symbol corresponds to a different excluded conservation law I_q^+ (the legend indicates the value of q). The distance approaches zero for even q, whereas it remains finite for odd q, in agreement with the discussion of Sec. VI. The lines are the distances from the corresponding defective generalized Gibbs ensemble $\rho_{\mathrm{dGGE}}^{(+q)}$ with maximal entanglement entropy.

2. More local conservation laws are more important

On the other hand, for odd q we find that $\mathcal{D}_\infty^{\mathrm{d}(+q),y}$ approaches constant values when y becomes large. This value agrees with the distance between the GGE and the defective GGE with maximal entanglement entropy (we stress that for the considered quench the defective GGE does not always correspond to a stationary point of the entanglement entropy under a variation of the excluded integral of motion, as shown in Fig. 20 of Appendix D).

The fact that $\mathcal{D}_\infty^{\mathrm{d}(+q),y}$ tends to a constant at large y shows that retaining an infinite number of local conservation laws while excluding one of them is insufficient for describing the stationary state. By comparing distances for different values of q we observe that for a given value of y, $\mathcal{D}_\infty^{\mathrm{d}(+q),y}$ decreases as a function of q. This implies *the more local the conservation law, the more important it is for describing the stationary state*.

XI. QUENCHES FROM THE FERROMAGNETIC PHASE: EFFECTS OF SPONTANEOUS SYMMETRY BREAKING

We now turn to quenches originating in the ferromagnetic phase, i.e., $h_0 < 1$. In this case, the time evolved initial state is given by

$$|\Psi_t\rangle = \frac{|\psi_t\rangle_{\mathrm{R}} + |\psi_t\rangle_{\mathrm{NS}}}{\sqrt{2}}, \qquad |\psi_t\rangle_a = e^{-iH_a t}\,|0;h_0\rangle_a\,, \quad a = \mathrm{R,NS} \tag{11.1}$$

where $|0;h_0\rangle_{\mathrm{R/NS}}$ are the ground states of the Hamiltonian $H(h_0)$ with periodic/antiperiodic boundary conditions. In order to analyze reduced density matrices after a quantum quench from the ferromagnetic phase we will make use of the following facts:

(a) The fermion parity $e^{i\pi\mathcal{N}} = \prod_j \sigma_j^z$ [Eq. (2.4)] is fully factorized in space.

(b) The states $|\psi_t\rangle_{\mathrm{R}}$ and $|\psi_t\rangle_{\mathrm{NS}}$ are eigenstates of $e^{i\pi\mathcal{N}}$ with eigenvalues 1 and -1, respectively.

(c) The difference between the expectation values of local operators in the states $|\psi_t\rangle_{\mathrm{R}}$ and $|\psi_t\rangle_{\mathrm{NS}}$ tends to zero in the thermodynamic limit.

(d) The RDMs $\mathrm{Tr}_{\bar{A}}\,[|\psi_t\rangle_{\mathsf{aa}}\langle\psi_t|]$, $\mathsf{a} = \mathrm{R,NS}$, where A is a single interval and $\bar{A}$ its complement, are Gaussian.

Property (b) allows us to express the full density matrix in the form [cf. Eq. (7.1)]

$$\rho(t) = \frac{1}{Z}\Bigg\{\sum_{\mathcal{O}_e}[{}_{\mathrm{R}}\langle\psi_t|\mathcal{O}_e|\psi_t\rangle_{\mathrm{R}} + {}_{\mathrm{NS}}\langle\psi_t|\mathcal{O}_e|\psi_t\rangle_{\mathrm{NS}}]\mathcal{O}_e + \sum_{\mathcal{O}_o} 2\,\mathrm{Re}[\langle\mathcal{O}_o\rangle_{\mathrm{NS}}\langle\psi_t|\mathcal{O}_o|\psi_t\rangle_{\mathrm{R}}]\mathcal{O}_o\Bigg\}, \tag{11.2}$$

where Z ensures that $\mathrm{Tr}[\rho(t)] = 1$ and $\{\mathcal{O}_e\} \cup \{\mathcal{O}_o\}$ is a complete set of Hermitian involutions with the property

$$[e^{i\pi\mathcal{N}},\mathcal{O}_e] = 0, \qquad \{e^{i\pi\mathcal{N}},\mathcal{O}_o\} = 0. \tag{11.3}$$

We will refer to $\mathcal{O}_{e/o}$ as even and odd operators, respectively. The main difference between even and odd operators is that the latter are not local in terms of fermions: a Jordan-Wigner string is attached to them. We are interested in the RDM of a block A of ℓ contiguous spins, which is obtained by tracing out the degrees of freedom outside A:

$$\rho_\ell = \mathrm{Tr}_{\bar{A}}[\rho]. \tag{11.4}$$

A convenient representation for ρ_ℓ is obtained by restricting the sums in Eq. (11.2) to involutions that act as the identity operator outside the interval A, i.e.,

$$\mathcal{O} \to \mathcal{O}^{(A)} \otimes \mathrm{I}^{(\bar{A})}, \tag{11.5}$$

where the superscript (A) indicates that the operators act on the Hilbert space over all sites in A. As a result of property (a), fermion parity has a simple restriction onto the interval A,

$$e^{i\pi\mathcal{N}_A} \equiv \prod_{l\in A}\sigma_l^z, \tag{11.6}$$

and can be used to subdivide operators $\mathcal{O}^{(A)}$ into even and odd ones

$$\left[e^{i\pi\mathcal{N}_A},\mathcal{O}_e^{(A)}\right] = 0, \qquad \left\{e^{i\pi\mathcal{N}_A},\mathcal{O}_o^{(A)}\right\} = 0. \tag{11.7}$$

This then implies that we can decompose the RDMs of (11.2) into even and odd parts as well:

$$\rho_\ell = \rho_{\ell,e} + \rho_{\ell,o}. \tag{11.8}$$

In the thermodynamic limit we then may employ property (c) to obtain the following expressions:

$$\rho_{\ell,e}(t) = \frac{1}{2^\ell}\sum_{\mathcal{O}_e} {}_{\mathrm{R}}\langle\psi_t|\mathcal{O}_e|\psi_t\rangle_{\mathrm{R}}\mathcal{O}_e, \qquad \rho_{\ell,o}(t) = \frac{1}{2^\ell}\sum_{\mathcal{O}_o}\mathrm{Re}[{}_{\mathrm{NS}}\langle\psi_t|\mathcal{O}_o|\psi_t\rangle_{\mathrm{R}}]\mathcal{O}_o. \tag{11.9}$$

Importantly, the even part $\rho_{\ell,e}(t)$ is Gaussian (7.7) by virtue of property (d), and has the same structure as RDMs for quenches originating in the paramagnetic phase. On the other hand, the odd part $\rho_{\ell,o}$ has its origin in the spontaneous breaking of the $\mathbb{Z}_2$ symmetry. The commutation relations (11.7) imply that $\mathrm{Tr}[\rho_{\ell,o}(t)\rho_\ell^{\mathrm{Ga}}] = 0$ for any Gaussian density matrix ρ_ℓ^{Ga} because the latter is by construction even. As a result, the odd part $\rho_{\ell,o}$ of the RDM enters the distance from a Gaussian state only through its norm

$$\mathcal{D}\big(\rho_\ell(t),\rho_\ell^{\mathrm{Ga}}\big) = \sqrt{\frac{\big\|\rho_{\ell,e}(t) - \rho_\ell^{\mathrm{Ga}}\big\|_F^2 + \|\rho_{\ell,o}(t)\|_F^2}{\|\rho_{\ell,e}\|_F^2 + \|\rho_{\ell,o}\|_F^2 + \big\|\rho_\ell^{\mathrm{Ga}}\big\|_F^2}}. \tag{11.10}$$

We will be interested in the cases where ρ_ℓ^{Ga} describe Gibbs or (truncated) generalized Gibbs ensembles. The Frobenius norms $\|\rho_{\ell,e}(t) - \rho_\ell^{\mathrm{Ga}}\|_F$, $\|\rho_{\ell,e}\|_F$, and $\|\rho_\ell^{\mathrm{Ga}}\|_F$ can be efficiently evaluated by means of Eq. (8.33). What remains in order to determine the distance (11.10) is a method for calcuating the Frobenius norm $\|\rho_{\ell,o}\|_F$. This is a somewhat involved technical problem, which is addressed in Sec. XI A and Appendix B. The basic idea is to utilize a cluster decomposition theorem at any finite time after the quench (see also Ref. 36).

A. $\|\rho_{\ell,o}\|_F$ from cluster decomposition

The main difficulty in calculating the Frobenius norm of $\rho_{\ell,o}$ is that the latter is not Gaussian. The idea is therefore to

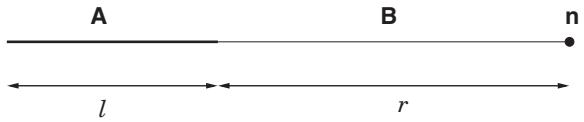

FIG. 10. Geometry of the composite system $A \cup n$ used in calculating $\|\rho_{\ell,o}\|_F$, where ρ_ℓ is the RDM of subsystem A. The single site at position n is separated from A by a block B of length r.

obtain $\rho_{\ell,o}$ as a reduction of a Gaussian operator. To that end, we consider a composite system $C = A \cup n$ consisting of our subsystem A and a single site at position n, which is separated from A by a block B of length r (see Fig. 10).

The even part of the RDM $\rho_C(t)$ can be expanded in a complete basis of Hermitian involutions $\mathcal{O}_{e/o}$ as

$$\rho_{C,e}(t) = \frac{1}{2^{\ell+1}}\left[\sum_{\mathcal{O}_e}\langle \mathcal{O}_e\sigma_n^z\rangle\, \mathcal{O}_e\sigma_n^z + \sum_{\mathcal{O}_o}\sum_{\alpha=x,y}\langle \mathcal{O}_o\sigma_n^\alpha\rangle\, \mathcal{O}_o\sigma_n^\alpha\right], \tag{11.11}$$

where $\langle\ldots\rangle = \langle\Psi_t|\ldots|\Psi_t\rangle \approx {}_{\rm R}\langle\psi_t|\ldots|\psi_t\rangle_{\rm R}$, since both $\mathcal{O}_e\sigma_n^z$ and $\mathcal{O}_o\sigma_n^\alpha$ in (11.11) are even operators with respect to fermion parity. In the limit of large separation r, we may use the cluster decomposition principle to simplify the expectation values

$$\langle \mathcal{O}_e\sigma_n^z\rangle \overset{r\to\infty}{\to} \langle\mathcal{O}_e\rangle\langle\sigma_n^z\rangle, \quad \langle \mathcal{O}_o\sigma_n^\alpha\rangle \overset{r\to\infty}{\to} \langle\mathcal{O}_o\rangle\langle\sigma_n^\alpha\rangle. \tag{11.12}$$

This then leads to the following relation between RDMs in the limit or large separation:

$$\lim_{r\to\infty}\rho_{C,e}(t) = \rho_{\ell,e}(t)\otimes\rho_{1,e}(t) + \rho_{\ell,o}(t)\otimes\rho_{1,o}(t), \tag{11.13}$$

where ρ_1 is the RDM of site n. The piece of interest to us is

$$\rho_{\ell,o}\otimes\rho_{1,o} = \lim_{r\to\infty}\frac{1}{2^{\ell+1}}\sum_{\mathcal{O}_o}\sum_{\alpha=x,y}\langle\mathcal{O}_o\sigma_n^\alpha\rangle\,\mathcal{O}_o\sigma_n^\alpha. \tag{11.14}$$

In the next step we move from spins to Majorana fermions by means of the Jordan-Wigner transformation (2.2):

$$\rho_{\ell,o}\otimes\rho_{1,o} = \lim_{r\to\infty}\frac{1}{2^{\ell+1}}\sum_{\substack{\mathcal{A}_o\\ \alpha=x,y}}\langle a_n^\alpha\mathcal{A}_o^\dagger e^{i\pi\mathcal{N}_B}\rangle\,\mathcal{A}_o e^{i\pi\mathcal{N}_B}a_n^\alpha, \tag{11.15}$$

where $\mathcal{A}_o$ are odd products of Majorana fermions acting on sites within A. Importantly, the fermionic expression (11.15) depends on the configuration of Majoranas in subsystem B through the Jordan-Wigner string operator. The right-hand side of (11.15) can be cast in the form

$$\rho_{\ell,o}\otimes\rho_{1,o} = \lim_{r\to\infty}\langle e^{i\pi\mathcal{N}_B}\rangle\, e^{i\pi\mathcal{N}_B}\frac{\mathfrak{p}-\sigma_n^z\mathfrak{p}\sigma_n^z}{2}, \tag{11.16}$$

where $\mathfrak{p}$ is a normalized, Gaussian operator (7.7) acting on the Hilbert space over sites $A\cup n$:

$$\mathfrak{p} \equiv \frac{{\rm Tr}_{\overline{A\cup n}}[e^{i\pi\mathcal{N}_B}|\psi_t\rangle_{\rm RR}\langle\psi_t|]}{\langle e^{i\pi\mathcal{N}_B}\rangle}. \tag{11.17}$$

In writing (11.15) we are assuming $\langle e^{i\pi\mathcal{N}_B}\rangle \neq 0$. The fact that $\mathfrak{p}$ is Gaussian is a consequence of the particular form of $|\psi_t\rangle_{\rm R}$ [which is the analog of (2.13) in the R sector] and $\mathcal{N}_B$ being quadratic in fermions. The odd part of the single-site RDM is of the form

$$\rho_{1,o}(t) = m^x(t)\sigma_n^x + m^y(t)\sigma_n^y, \tag{11.18}$$

and hence

$$[\rho_{1,o}(t)]^2 = ([m^x(t)]^2 + [m_y(t)]^2){\rm I}_2 \equiv m_\perp^2(t){\rm I}_2. \tag{11.19}$$

Here the late-time behavior of $m^{x,y}(t)$ is given by (9.14) and (9.15), respectively, and following Ref. 31 they can be easily calculated numerically for all times. Combining (11.19) and (11.16) we obtain

$$\begin{aligned}\|\rho_{\ell,o}\|_F &= \lim_{r\to\infty}\frac{|\langle e^{i\pi\mathcal{N}_B}\rangle|}{\sqrt{2}|m_\perp(t)|}\left\|\frac{\mathfrak{p}-\sigma_n^z\mathfrak{p}\sigma_n^z}{2}\right\|_F\\ &= \lim_{r\to\infty}\frac{|\langle e^{i\pi\mathcal{N}_B}\rangle|}{2|m_\perp(t)|}\sqrt{{\rm Tr}\big[\mathfrak{p}^2-\big(\sigma_n^z\mathfrak{p}\big)^2\big]}.\end{aligned} \tag{11.20}$$

Since both $\mathfrak{p}$ and $\sigma_n^z\mathfrak{p}\sigma_n^z$ are Gaussian, their moments can be written in terms of their respective correlation matrices

$$\mathcal{G}_{ij} \equiv {\rm Tr}[\mathfrak{p}a_ja_i] - \delta_{ij}, \quad \bar{\mathcal{G}}_{ij} \equiv {\rm Tr}\left[\sigma_n^z\mathfrak{p}\sigma_n^z a_ja_i\right] - \delta_{ij}. \tag{11.21}$$

We note that the correlation matrices are related by $\bar{\mathcal{G}} = P_n\mathcal{G}P_n$, with P_n the diagonal matrix that changes the sign of the last 2×2 block (I_d is the $d\times d$ identity)

$$P_n = {\rm I}_{2\ell}\oplus(-{\rm I}_2). \tag{11.22}$$

Using (8.32) we have

$${\rm Tr}[\mathfrak{p}^2] = \{\mathcal{G},\mathcal{G}\}, \quad {\rm Tr}\big[\big(\sigma_n^z\mathfrak{p}\big)^2\big] = \{\mathcal{G},\bar{\mathcal{G}}\}. \tag{11.23}$$

A slight complication arises because $\mathfrak{p}$ is not positive semidefinite. To account for this we must use the more general definition of $\{\Gamma,\Gamma'\}$ as the product of the eigenvalues of $(1+\Gamma\Gamma')/2$ with halved degeneracy.[60] We may then recast (11.20) in the form

$$\|\rho_{\ell,o}\|_F = \lim_{r\to\infty}\frac{|\langle e^{i\pi\mathcal{N}_B}\rangle|}{2|m_\perp(t)|}\sqrt{\{\mathcal{G},\mathcal{G}\}-\{\mathcal{G},\bar{\mathcal{G}}\}}. \tag{11.24}$$

While formally correct, (11.24) is not suitable for numerical computations, because at large distances $\langle e^{i\pi\mathcal{N}_B}\rangle$ becomes very close to zero. A more convenient expression derived in Appendix B is

$$\|\rho_{\ell,o}\|_F = \lim_{r\to\infty}\frac{\sqrt{\det({\rm I}_{2\ell}\oplus 0_{2r}\oplus{\rm I}_2 + i\Gamma_{A\cup B\cup n})}}{2^{1+\ell/2}|m_\perp(t)|}. \tag{11.25}$$

Here $\Gamma_{A\cup B\cup n}$ is the correlation matrix of the interval $A\cup B\cup n$ and is given by (7.4), (7.5), and (7.22). In order to utilize (11.25), we in principle have to consider infinite separations r and hence infinitely large matrices.

Crucially, in practice a *finite* separation $r > 2v_{\max}t$, where $v_{\max} = \max_k\epsilon_h'(k)$ is the maximal propagation velocity, is sufficient to recover the $r\to\infty$ limit up to corrections that are exponentially small in r/ξ. Here ξ is the correlation length in the initial state. A representative example is shown in Fig. 11. In practice, using a finite $r > 2v_{\max}t + \xi\delta$ with $\delta\approx 20$ provides an efficient way for calculating $\|\rho_{\ell,o}(t)\|_F$ and then by means of (11.10) distances $\mathcal{D}(\rho_\ell(t),\rho_\ell^{\rm Ga})$ for quenches originating in the ferromagnetic phase.

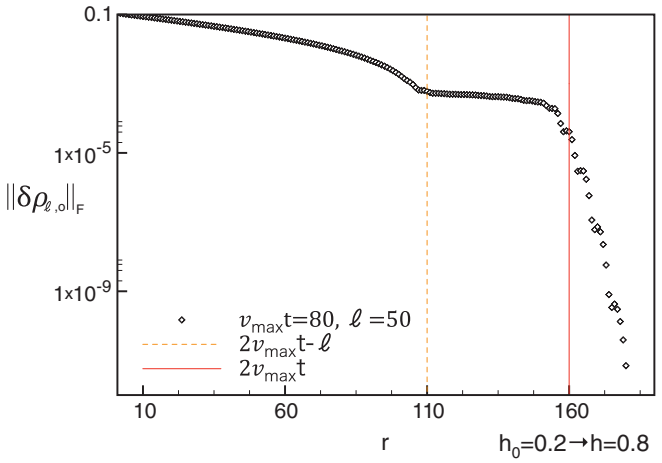

FIG. 11. (Color online) Difference $\|\delta\rho_{\ell,o}\|_F = \|\rho_{\ell,o}\|_F - \lim_{r\to\infty} \|\rho_{\ell,o}\|_F$ as a function of the separation r for a quench from $h_0 = 0.2$ to $h = 0.8$. We see that for $r > 2v_{\max}t$ the difference becomes exponentially small in r/ξ, where ξ is the correlation length in the initial state.

B. Results for quenches from the ferromagnetic phase

For quenches with $h_0 < 1$ and in the thermodynamic limit, we determine the distance between the quench RDM and that of an appropriate thermal or generalized Gibbs ensemble by means of relations (11.10) and (11.25). The correlation matrices for all cases are of the form (7.4), (7.5) with elements given in (7.12), (7.14), and (7.22), respectively. For a subsystem of size ℓ most terms require the calculation of determinants of $2\ell \times 2\ell$ matrices, which is easily done numerically. The evaluation of $\|\rho_{\ell,o}\|_F$ is significantly more costly, and in practice involves determinants of at most $2(\ell + 2v_{\max}t + \xi\delta) \times 2(\ell + 2v_{\max}t + \xi\delta)$ matrices, as discussed above.

Results for a quench from $h_0 = \frac{1}{3}$ to $\frac{2}{3}$ and subsystem sizes $\ell = 10,20,30,\ldots,150$ are shown in Figs 12 and 13. We see that the distance between quench and Gibbs RDMs tends to a

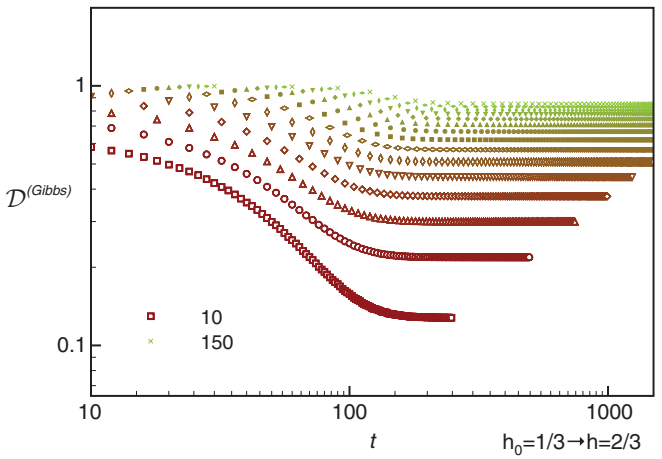

FIG. 12. (Color online) Distance $\mathcal{D}^{\rm Gibbs} = \mathcal{D}(\rho_\ell(t), \rho_\ell^\beta)$ after a quench within the ferromagnetic phase for subsystem sizes $\ell = 10,20,\ldots,150$. As ℓ increases, the color fades from brown to green, the symbols become smaller, and the curves narrower. At late times the distances tend to constants depending on subsystem size.

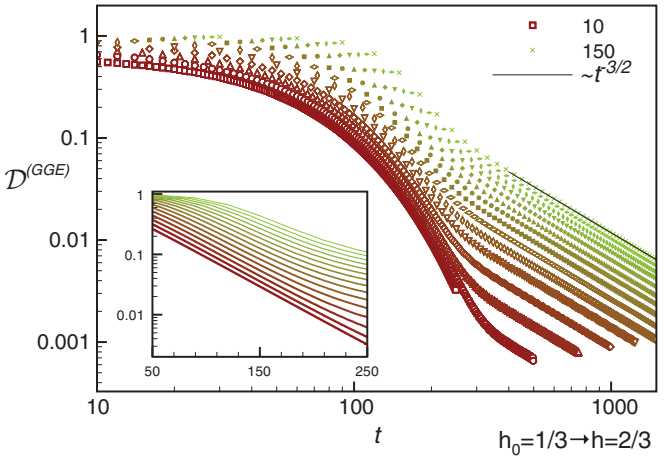

FIG. 13. (Color online) Distance $\mathcal{D}^{\rm GGE} = \mathcal{D}(\rho_\ell(t), \rho_\ell^{\rm GGE})$, after a quench within the ferromagnetic phase for the subsystem lengths $\ell = 10,20,\ldots,150$. We used the same notations of Fig. 3. The behavior is almost the same as that shown in Figs. 3 and 5, but the effect of the spontaneous magnetization is visible at intermediate times, when the distance decays exponentially (inset).

ℓ-dependent constant at late times. On the other hand, as shown in Fig. 13, at sufficiently late times the distance between $\rho_\ell(t)$ and $\rho_{{\rm GGE},\ell}$ decays to zero in a universal power-law fashion

$$\mathcal{D}(\rho_\ell(t), \rho_{{\rm GGE},\ell}) \overset{Jt\gg 1}{\to} k(\ell)(Jt)^{-3/2} + \cdots . \qquad (11.26)$$

The large-ℓ asymptotics of the function $k(\ell)$ can be inferred in the same way as for quenches within the paramagnetic phase. On surfaces with constant, small $\mathcal{D}$, time scales as $t \sim \ell^{4/3}$ as is shown in Fig. 14, which implies that

$$k(\ell) \sim \ell^2 . \qquad (11.27)$$

We conclude that the late-time behavior of the distance between quench and generalized Gibbs RDMs is the same as for quenches within the paramagnetic phase. The mean relaxation time $t^*_{\rm rms}$ is therefore again given by (10.7).

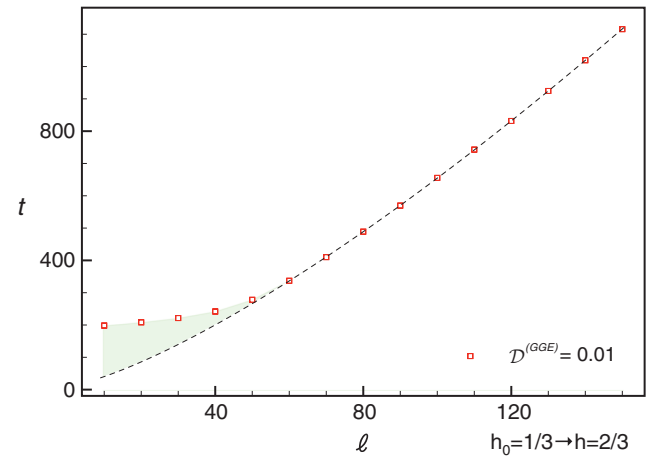

FIG. 14. (Color online) The time vs the subsystem length at fixed distance $\mathcal{D}(\rho_\ell(t), \rho_\ell^{\rm GGE}) = 0.01$ (black solid line of the left plot). The dashed curve is $t = a + b\ell^{4/3}$, with a and b obtained by fitting the numerical data. The filled region shows the effect of the spontaneous magnetization.

Interestingly, this coincides with the result obtained in Ref. 32 for the relaxation of the order parameter two-point function after quenches within the ferromagnetic phase. The effects of the spontaneous symmetry breaking are important only at short and intermediate times. It is shown in the inset of Fig. 13 that there is a time window, in which the odd part of the RDM gives the dominant contribution to the distance, which decays exponentially.

C. Magnitude of the contribution due to $\rho_{\ell,o}$

The effects of the spontaneously broken $\mathbb{Z}_2$ symmetry in the initial state make themselves felt through the $\mathbb{Z}_2$-odd part $\rho_{\ell,o}$ of the density matrix. The relative importance of $\rho_{\ell,o}$ for large ℓ can be estimated by considering the von Neumann entropy of subsystem A

$$S_{\rm vN}[\rho_\ell] = {\rm Tr}\,[\rho_\ell \ln(\rho_\ell)]\,. \tag{11.28}$$

We recall that the von Neumann entropy after a global quench grows linearly in time until the Fermi time $t_F = \ell/(2v_{\rm max})$, and then saturates to a value proportional to the subsystem size ℓ.[66,67] Using the commutation relations (11.8) we see that the even part $\rho_{\ell,e}$ can be expressed in terms of the full RDM ρ_ℓ as

$$\rho_{\ell,e} = \frac{\rho_\ell + e^{i\pi\mathcal{N}_A}\rho_\ell e^{i\pi\mathcal{N}_A}}{2}. \tag{11.29}$$

Since for any set of density matrices ρ_i the von Neumann entropy satisfies[68] ($\lambda_i > 0$, $\sum_i \lambda_i = 1$)

$$\sum_i \lambda_i \ln\lambda_i \leqslant S_{\rm vN}\left[\sum_i \lambda_i \rho_i\right] - \sum_i \lambda_i S_{\rm vN}[\rho_i] \leqslant 0\,, \tag{11.30}$$

the following bounds on the von Neumann entropy of subsystem A hold:

$$S_{\rm vN}[\rho_{\ell,e}] - \ln 2 \leqslant S_{\rm vN}[\rho_\ell] \leqslant S_{\rm vN}[\rho_{\ell,e}]. \tag{11.31}$$

This demonstrates that at any time after the quench the symmetry breaking contribution to the von Neumann entropy will be at most $\ln 2$. Given that for large subsystems the von Neumann entropy at late times is proportional to ℓ, we conclude that the relative contribution of the odd part of the RDM will be important only for small subsystem sizes.

1. A conjecture for $\|\rho_{\ell,o}\|_F$ in the limit of large ℓ and Jt

We now consider the *space-time scaling limit*[31]

$$\ell, Jt \to \infty\,, \quad \frac{\ell}{Jt} \text{ fixed.} \tag{11.32}$$

We observe that in this limit our numerical results for quenches within the ferromagnetic phase are in excellent agreement with the following relation:

$$\ln\|\rho_{\ell,o}(t)\|_F \approx \ln\|\rho_{\ell,e}(t)\|_F + \int_0^\pi \frac{dk}{2\pi}\ln(\cos\Delta_k) \times \max_k\{0, 2\varepsilon_k' t - \ell + \mathcal{O}(\ell^0,t^0)\}. \tag{11.33}$$

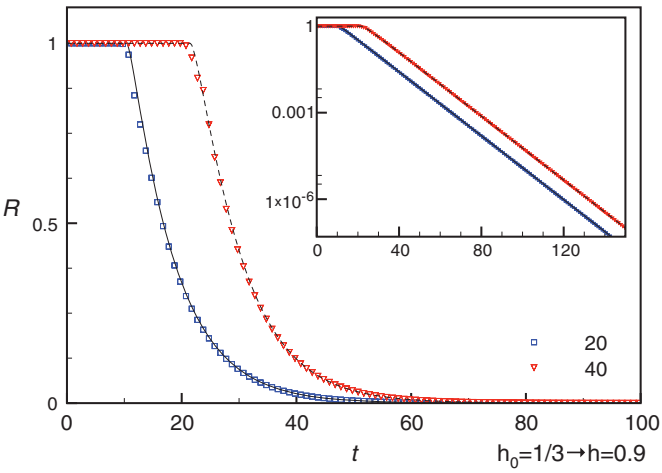

FIG. 15. (Color online) The ratio $R = \frac{\|\rho_{\ell,o}(t)\|_F}{\|\rho_{\ell,e}(t)\|_F}$ after a quench within the ferromagnetic phase for subsystem lengths $\ell = 10,20$. The lines correspond to the analytic expression (11.33), where we have included a correction $\mathcal{O}(\ell^0)$ by shifting $\ell \to \ell - 1.2$. The inset presents the same data on a logarithmic scale.

Here we have highlighted the asymptotic nature of the relation and indicated by $\mathcal{O}(\ell^0,t^0)$, where the most important corrections will arise. Since $\ln\|\rho_{\ell,e}(t)\|_F$ is proportional to the Rényi entropy S_2 [cf. Eq. (8.13)], we may use the known results[66] on the asymptotics of the latter

$$\ln\|\rho_{\ell,e}(t)\|_F = -S_2/2 \approx \int_0^\pi \frac{dk}{2\pi}\ln\frac{1+\cos^2\Delta_k}{2}\min(2\varepsilon_k' t, \ell) + \mathcal{O}(\ell^0,t^0). \tag{11.34}$$

Combining (11.34) and (11.33) provides a conjecture for the asymptotic behavior of $\|\rho_{\ell,o}\|_F$. This conjecture is compared to numerical results in Fig. 15. The agreement is clearly quite good.

XII. QUENCHES ACROSS THE CRITICAL POINT

We now turn to quenches across the critical point. These are of particular interest.[14,31,42] In Fig. 16 we plot the distance between quench and GGE reduced density matrices for a quench from the ferromagnetic phase ($h_0 = \frac{1}{2}$) to the paramagnetic phase ($h = \frac{3}{2}$). The 15 data sets displayed correspond to subsystem sizes between $\ell = 10$ and 150. We find that the distance $\mathcal{D}^{\rm GGE} = \mathcal{D}(\rho_\ell(t), \rho_\ell^{\rm GGE})$ again decays in a universal $t^{-3/2}$ power law. In Fig. 17 we consider the same quench, but focus on very small subsystem sizes $\ell = 1,2,3,4$. We observe that the distance displays an oscillatory behavior on top of a power-law decay in time. This is in agreement with the analytic results discussed in Sec. IX B for the $\ell = 1$ case. Increasing the subsystem size leads to a rapid suppression of the amplitude of the oscillations.

In Figs 18 and 19 we consider the reverse quenches, i.e., starting at $h_0 = \frac{3}{2}$ in the paramagnetic phase, and quenching to $h = \frac{1}{2}$ in the ferromagnetic phase. The behavior of the distances is very similar to what we found for the quench from $h_0 = \frac{1}{2}$ to $h = \frac{3}{2}$: at late times the distance decays as a

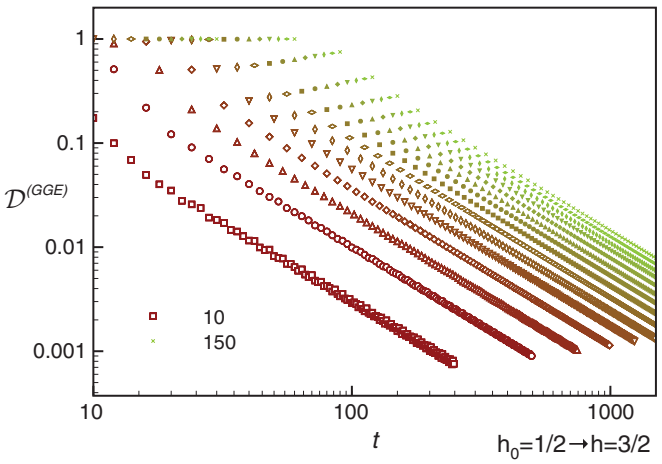

FIG. 16. (Color online) Distance $\mathcal{D}^{\rm GGE} = \mathcal{D}(\rho_\ell(t), \rho_\ell^{\rm GGE})$, after a quench from ferromagnetic phase to the paramagnetic phase for the subsystem lengths $\ell = 10,20,\ldots,150$. The conventions are the same as in Fig. 3.

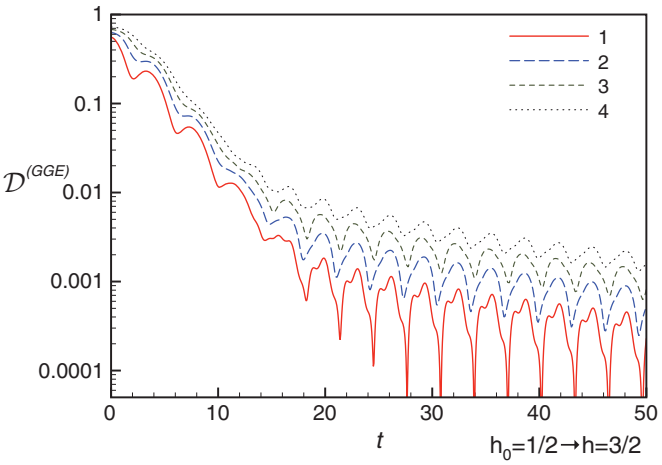

FIG. 17. (Color online) Distance $\mathcal{D}^{\rm GGE} = \mathcal{D}(\rho_\ell(t), \rho_\ell^{\rm GGE})$, after a quench from ferromagnetic phase to the paramagnetic phase for the small subsystems $\ell = 1,2,3,4$.

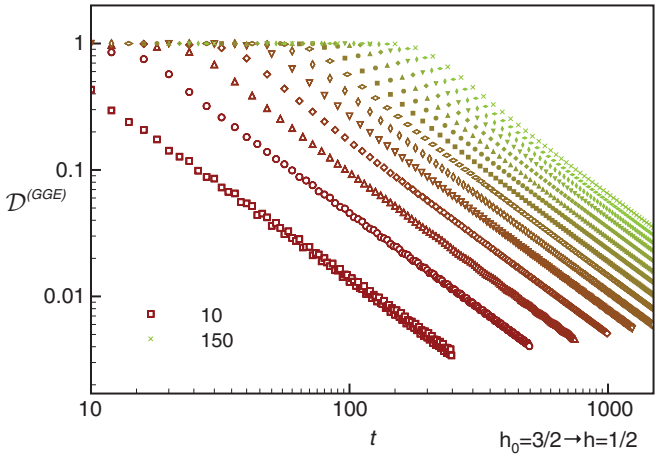

FIG. 18. (Color online) Distance $\mathcal{D}(\rho_\ell(t), \rho_\ell^{\rm GGE})$, after a quench from paramagnetic phase to the ferromagnetic phase for the subsystem lengths $\ell = 10,20,\ldots,150$. The conventions are the same as in Fig. 3.

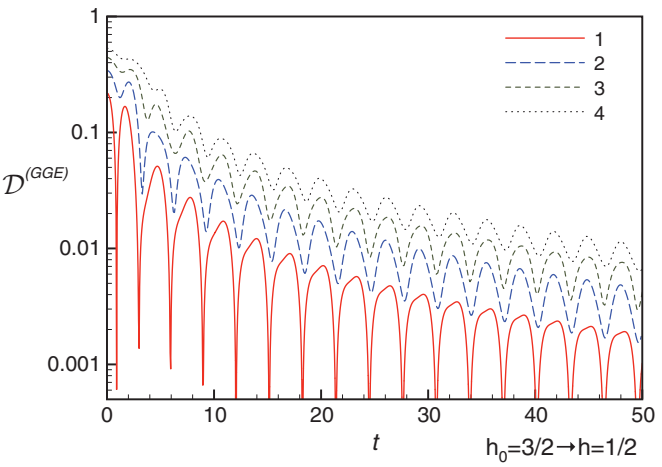

FIG. 19. (Color online) Distance $\mathcal{D}(\rho_\ell(t), \rho_\ell^{\rm GGE})$, after a quench from paramagnetic phase to the ferromagnetic phase for the small subsystems $\ell = 1,2,3,4$.

$t^{-3/2}$ power law, and for small subsystem sizes we observe oscillatory behavior on top of this decay.

XIII. SUMMARY AND CONCLUSIONS

In this work we have considered the evolution of reduced density matrices after a quantum quench in the transverse-field Ising chain. The main result of our work is to demonstrate that

$$\lim_{t\to\infty} \rho_\ell(t) = \rho_{{\rm GGE},\ell}, \tag{13.1}$$

where $\rho_\ell(t)$ is the reduced density matrix of a subsystem consisting of ℓ adjacent spins after a quench of the transverse field, and $\rho_{{\rm GGE},\ell}$ is the reduced density matrix of an appropriately defined generalized Gibbs ensemble. The derivation of (13.1) is based on defining an appropriate distance $\mathcal{D}(\rho,\rho')$ on the space of reduced density matrices, and then establishing that the distance between quench and GGE reduced density matrices approaches zero at late times. For our particular choice of distance we found that at late times this distance approaches zero as a universal power law in time

$$\mathcal{D}(\rho_\ell(t), \rho_{{\rm GGE},\ell}) \sim t^{-3/2}. \tag{13.2}$$

We have presented a detailed construction of $\rho_{{\rm GGE},\ell}$ in terms of the *local* (in space) integrals of motion $I_n^\pm$ of the TFIC. The densities of these conservation laws involve only spins on $n+2$ consecutive sites. We proved that these local conservation laws are related in a *linear* fashion to the occupation numbers of the Bogoliubov fermions that diagonalize the Hamiltonian of the TFIC. This linear relation establishes the equivalence of our construction of the GGE to the one frequently used in the literature, which is based on mode occupation numbers.

We then have addressed the question as to which of the conservation laws are most important for obtaining an accurate description of the stationary limit $\lim_{t\to\infty}\rho_\ell(t)$ of the quench RDM. To that end, we introduced (defective) truncated generalized Gibbs ensembles, which are missing some of the local conservation laws. We found that the more local the conservation laws (i.e., the fewer consecutive spins their densities involve), the more important they are for describing the stationary state of a given subsystem. Loosely speaking,

we observed that in order to obtain a good description of the stationary state RDM of a subsystem of size ℓ, we need to retain all local conservation laws, whose densities involve at most $\approx \ell + n_0$ neighboring spins, where n_0 is a constant depending on h_0 and h. Leaving out "highly local" conservation laws generally provides a very poor description of the stationary state. We believe that this interesting connection between locality of conservation laws and their importance in the GGE context is not restricted to the transverse field Ising chain, but will hold more generally for quantum quenches in integrable models.

Our work raises a number of issues. First and foremost is the dependence of the results obtained on the precise definition of the distance on the space of reduced density matrices. We have argued that the "best" distance is the one based on the trace norm because it provides the most direct and precise information on the time evolution of local observables. Unfortunately, this distance is much harder to handle analytically. It would however be very interesting to implement it in purely numerical studies using iTEBD or related algorithms.

ACKNOWLEDGMENTS

We thank P. Calabrese and J. Eisert for helpful discussions. This work was supported by the EPSRC under Grants No. EP/I032487/1 and No. EP/J014885/1 and the National Science Foundation under Grant No. NSF PHY11-25915 (F.H.L.E.). F.H.L.E. is grateful to the KITP in Santa Barbara for hospitality.

APPENDIX A: INEQUALITIES INVOLVING THE FROBENIUS NORM OF RDMS FOR SPIN-$\frac{1}{2}$ QUANTUM SPIN CHAINS

In this Appendix we provide lower and upper bounds for the Frobenius norm of the difference of two reduced density matrices $\|\rho - \rho'\|_F$ in a translationally invariant system. An upper bound is obtained as follows:

$$\begin{aligned}\|\rho-\rho'\|_F^2 &= \mathrm{Tr}[\rho^2+\rho'^2-2\rho\rho'] \\ &= \|\rho\|_F^2+\|\rho'\|_F^2-2\,\mathrm{Tr}(\rho\rho') \\ &\leqslant \|\rho\|_F^2+\|\rho'\|_F^2. \end{aligned} \tag{A1}$$

Here we have used that both ρ and ρ' are positive semidefinite and hence

$$\begin{aligned}\mathrm{Tr}(\rho\rho') &= \sum \lambda_j \rho'_{jj} \geqslant \lambda_{\min}\sum_j \rho'_{jj} \\ &= \lambda_{\min}\mathrm{Tr}\rho' = \lambda_{\min} \geqslant 0, \end{aligned} \tag{A2}$$

where $0 \leqslant \lambda_{\min} \leqslant \lambda_j$ are the eigenvalues of ρ. To derive a lower bound we start by expressing the RDM of a block of ℓ spins in a spin-$\frac{1}{2}$ chain in the form

$$\rho_\ell = \frac{1}{2^\ell}\sum_{\{\alpha_j\}} \mathrm{Tr}\left[\rho\,\sigma_1^{\alpha_1}\dots\sigma_\ell^{\alpha_\ell}\right]\sigma_1^{\alpha_1}\dots\sigma_\ell^{\alpha_\ell}, \tag{A3}$$

where $\alpha_i = 0,x,y,z$ with $\sigma^0 \equiv \mathrm{I}$, and ρ is the density matrix of the full system; ρ_ℓ is only function of the length because of translational invariance. By singling out the term with $\alpha_\ell = 0$, we can express this in the form

$$\rho_\ell = \frac{\rho_{\ell-1}\otimes \mathrm{I}}{2} + \sum_{\alpha_\ell=1}^{3}\delta\rho_{\ell-1}^{\alpha_\ell}\sigma_\ell^{\alpha_\ell}, \tag{A4}$$

where $\rho_{\ell-1}$ is the RDM of the block consisting of sites $1,\dots,\ell-1$. We also write the RDM of the ℓth spin

$$\rho_1 = \frac{\mathrm{I}}{2} + \sum_{\alpha_\ell=1}^{3}\mathrm{Tr}\left[\delta\rho_{\ell-1}^{\alpha_\ell}\right]\sigma_\ell^{\alpha_\ell} \tag{A5}$$

and observe that

$$\|\rho_1-\rho'_1\|_F^2 = 2\sum_{\alpha_\ell=1}^{3}\left(\mathrm{Tr}\left[\Omega_{\ell-1}^{\alpha_\ell}\right]\right)^2. \tag{A6}$$

Here we have defined $\Omega_{\ell-1}^{\alpha_\ell} = \delta\rho_{\ell-1}^{\alpha_\ell} - \delta\rho'^{\alpha_\ell}_{\ell-1}$. Using (A4) we have

$$\begin{aligned}\|\rho_\ell-\rho'_\ell\|_F^2 &= \frac{\|\rho_{\ell-1}-\rho'_{\ell-1}\|_F^2}{2} + 2\sum_{\alpha_\ell=1}^{3}\left\|\Omega_{\ell-1}^{\alpha_\ell}\right\|_F^2 \\ &\geqslant \frac{\|\rho_{\ell-1}-\rho'_{\ell-1}\|_F^2}{2} + \sum_{\alpha_\ell=1}^{3}\frac{\left(\mathrm{Tr}\left[\Omega_{\ell-1}^{\alpha_\ell}\right]\right)^2}{2^{\ell-2}} \\ &= \frac{\|\rho_{\ell-1}-\rho'_{\ell-1}\|_F^2}{2} + \frac{\|\rho_1-\rho'_1\|_F^2}{2^{\ell-1}}, \end{aligned} \tag{A7}$$

where we have used that for $N\times N$ matrices M we have $N\,\mathrm{Tr}M^2 \geqslant (\mathrm{Tr}M)^2$ in the second step, and (A6) in the last. Iterating Eq. (A7) $\ell-1$ times we obtain

$$\|\rho_\ell-\rho'_\ell\|_F^2 \geqslant 2^{1-\ell}\ell\|\rho_1-\rho'_1\|_F^2. \tag{A8}$$

This implies that for sufficiently large subsystem size ℓ, the distance $\|\rho_\ell-\rho'_\ell\|_F$ will generally be larger than $2^{1-\ell/2}$.

APPENDIX B: DERIVATION OF EQ. (11.25)

Our starting point is Eq. (11.24), i.e.,

$$\|\rho_{\ell,o}\|_F = \lim_{r\to\infty}\frac{|\langle e^{i\pi\mathcal{N}_B}\rangle|}{2|m_\perp(t)|}\sqrt{\{\mathcal{G},\mathcal{G}\}-\{\mathcal{G},\bar{\mathcal{G}}\}}. \tag{B1}$$

Our task is to evaluate

$$\langle e^{i\pi\mathcal{N}_B}\rangle^2\{\mathcal{G},\mathcal{G}\} \quad\text{and}\quad \langle e^{i\pi\mathcal{N}_B}\rangle^2\{\mathcal{G},\overline{\mathcal{G}}\}, \tag{B2}$$

where $\overline{\mathcal{G}} = P_n\mathcal{G}P_n$ and P_n is the diagonal involution defined in (11.22). We recall that $\{Q,Q_1\}$ denotes the product of the eigenvalues of $(\mathrm{I}+QQ_1)/2$ with halved degeneracy (the eigenvalues of QQ_1 are always double degenerate[69] for antisymmetric matrices Q and Q_1). The correlation matrix $\mathcal{G}$ defined in Eq. (11.21) turns out to be[60] the Schur complement of the block matrix Γ_B of the matrix $\Gamma_{A\cup B\cup n}$, i.e.,

$$\mathcal{G} = \Gamma_{A\cup n} - \Gamma_{A\cup n,\,B}\frac{1}{\Gamma_B}\Gamma_{B,\,A\cup n}. \tag{B3}$$

Here, $\Gamma_{R_1,\,R_2}$ denotes the matrix, whose rows and columns are associated with spatial regions R_1 and R_2, respectively, e.g.,

$$[\Gamma_{A\cup n,\,B}]_{ij} = \begin{cases}\Gamma_{i,j+2\ell}, & 0\leqslant i\leqslant 2\ell \\ \Gamma_{i+2r,j+2\ell}, & i>2\ell\,.\end{cases} \tag{B4}$$

Here, ℓ is the size of subsystem A, while r is the distance between A and site n (see Fig. 10).

The first step is to find determinant representations for $\{Q,Q\}$ and $\{Q,PQP\}$, where P is a generic symmetric involution ($P^2=\mathrm{I}$ and $P^t=P$).

We first consider $\{Q,Q\}$. Since Q is antisymmetric, its eigenvalues come in pairs $\pm q$:

$$0=\det|Q-q\mathrm{I}|=\det|Q^t-q\mathrm{I}|=\det|-Q-q\mathrm{I}|. \quad \text{(B5)}$$

Both eigenvalues $\pm q$ give rise to the same eigenvalue $1+q^2$ of $\mathrm{I}+Q^2$, and hence

$$\{Q,Q\}=\prod_{q\geqslant 0}\frac{1+q^2}{2}. \quad \text{(B6)}$$

Here the product is over all positive eigenvalues of Q (including half of the zero eigenvalues). Using that

$$\det|\mathrm{I}+iQ|=\prod_{q>0}(1+iq)\prod_{q>0}(1-iq)=\prod_{q>0}(1+q^2), \quad \text{(B7)}$$

it follows that

$$\{Q,Q\}=\det|(\mathrm{I}+iQ)/\sqrt{2}|\,. \quad \text{(B8)}$$

Next we consider $\{Q,PQP\}$. The matrix

$$P^{\frac{1}{2}}\equiv\frac{e^{i\pi/4}\mathrm{I}+e^{-i\pi/4}P}{\sqrt{2}} \quad \text{(B9)}$$

satisfies $(P^{\frac{1}{2}})^2=P$ and $(P^{\frac{1}{2}})^t=P^{\frac{1}{2}}$. Since we have

$$\mathrm{I}+QPQP=(P^{\frac{1}{2}})^{-1}[\mathrm{I}+(P^{\frac{1}{2}}QP^{\frac{1}{2}})^2]P^{\frac{1}{2}}, \quad \text{(B10)}$$

the eigenvalues of $\mathrm{I}+QPQP$ and $\mathrm{I}+(P^{\frac{1}{2}}QP^{\frac{1}{2}})^2$ coincide. Therefore,

$$\{Q,PQP\}=\{P^{\frac{1}{2}}QP^{\frac{1}{2}},P^{\frac{1}{2}}QP^{\frac{1}{2}}\}=\det\left|\frac{\mathrm{I}+iP^{\frac{1}{2}}QP^{\frac{1}{2}}}{\sqrt{2}}\right|, \quad \text{(B11)}$$

where in the last step we used Eq. (B8). Since $(P^{\frac{1}{2}})^2=P$ and $P^2=\mathrm{I}$, (B11) can be rewritten in the form

$$\{Q,PQP\}=\det|P|\det|(P+iQ)/\sqrt{2}|. \quad \text{(B12)}$$

Using (B8) and (B12), we can reexpress the quantities in (B2) as follows:

$$\begin{aligned}\langle e^{i\pi\mathcal{N}_B}\rangle^2\{\mathcal{G},\mathcal{G}\}&=\det|i\Gamma_B|\det|(\mathrm{I}+i\mathcal{G})/\sqrt{2}|,\\ \langle e^{i\pi\mathcal{N}_B}\rangle^2\{\mathcal{G},\overline{\mathcal{G}}\}&=\det|i\Gamma_B|\det|(P_n+i\mathcal{G})/\sqrt{2}|.\end{aligned} \quad \text{(B13)}$$

Here we have used that the expectation value of the string operator in region B is related to the correlation matrix Γ_B by $\langle e^{i\pi\mathcal{N}_B}\rangle^2=\det|i\Gamma_B|$. A remaining problem is that $\lim_{r\to\infty}\det|i\Gamma_B|=0$, which precludes a numerical evaluation of (B1) on the basis of expressions (B13). This complication is overcome as follows. We recall the expression of the determinant of a block matrix

$$\det\left|\begin{pmatrix}M_{11}&M_{12}\\M_{21}&M_{22}\end{pmatrix}\right|=\det|M_{22}|\det\left|M_{11}-M_{12}M_{22}^{-1}M_{21}\right|. \quad \text{(B14)}$$

We then substitute (B3) into (B13), and identify $2^{\ell+1}\langle e^{i\pi\mathcal{N}_B}\rangle^2\{\mathcal{G},\mathcal{G}\}$ and $2^{\ell+1}\langle e^{i\pi\mathcal{N}_B}\rangle^2\{\mathcal{G},\overline{\mathcal{G}}\}$ as the determinants of the matrices

$$\begin{pmatrix}\mathrm{I}+i\Gamma_{A\cup n}&i\Gamma_{A\cup n,B}\\i\Gamma_{B,A\cup n}&i\Gamma_B\end{pmatrix}\text{ and }\begin{pmatrix}P_n+i\Gamma_{A\cup n}&i\Gamma_{A\cup n,B}\\i\Gamma_{B,A\cup n}&i\Gamma_B\end{pmatrix}, \quad \text{(B15)}$$

respectively. Rearranging some of the rows and columns we obtain

$$\begin{aligned}\langle e^{i\pi\mathcal{N}_B}\rangle^2\{\mathcal{G},\mathcal{G}\}&=\frac{\det|\mathrm{I}_{2\ell}\oplus 0_{2r}\oplus\mathrm{I}_2+i\Gamma_{A\cup B\cup n}|}{2^{\ell+1}},\\ \langle e^{i\pi\mathcal{N}_B}\rangle^2\{\mathcal{G},\overline{\mathcal{G}}\}&=\frac{\det|\mathrm{I}_{2\ell}\oplus 0_{2r}\oplus(-\mathrm{I}_2)+i\Gamma_{A\cup B\cup n}|}{2^{\ell+1}}.\end{aligned} \quad \text{(B16)}$$

The representations (B16) are suitable for numerical calculations even in the limit of large r. There is one further simplification: in the limit $r\to\infty$ we have

$$\lim_{r\to\infty}\langle e^{i\pi\mathcal{N}_B}\rangle^2\{\mathcal{G},\overline{\mathcal{G}}\}=-\lim_{r\to\infty}\langle e^{i\pi\mathcal{N}_B}\rangle^2\{\mathcal{G},\mathcal{G}\}. \quad \text{(B17)}$$

To see this, we expand the determinants in (B16) with respect to the last 2×2 block (from here on we omit the subscript in $\Gamma_{A\cup B\cup n}$, i.e., $\Gamma\equiv\Gamma_{A\cup B\cup n}$)

$$\begin{aligned}&\det|\mathrm{I}_{2\ell}\oplus 0_{2r}\oplus\mathrm{I}_2+i\Gamma|+\det|\mathrm{I}_{2\ell}\oplus 0_{2r}\oplus(-\mathrm{I}_2)+i\Gamma|\\&\quad=2\det|\Gamma+i\mathrm{I}_{2\ell}\oplus 0_{2r+2}|-2\det|\Gamma_{A\cup B}+i\mathrm{I}_{2\ell}\oplus 0_{2r}|.\end{aligned} \quad \text{(B18)}$$

Using properties of the correlation matrix one could show that the determinants on the second line approach zero in the limit of large distance. For the sake of simplicity we propose a different proof, which is based on the assumption that the limit

$$\lim_{r\to\infty}\det|\Gamma_{A\cup B}+i\mathrm{I}_{2\ell}\oplus 0_{2r}| \quad \text{(B19)}$$

exists: we demonstrate that the limit can not be infinite, so the expression in Eq. (B18) does tend to zero as $r\to\infty$. To this end we consider the $(2\ell+2r)\times(2\ell+2r)$ correlation matrix G of a generic Gaussian density matrix, and show that the determinant $\det|G+i\mathrm{I}_{2\ell}\otimes 0_{2r}|$ has an upper bound independent of r. Hence, it can not diverge in the limit $r\to\infty$. Our proof is based on the following facts:

(a) $\|G\|_{op}\leqslant 1$, and hence $\|G^2\|_{op}\leqslant 1$ and $\|G+i\mathrm{I}_{2\ell}\otimes 0_{2r}\|_{op}\leqslant\|G\|_{op}+1\leqslant 2$;

(b) $G+i\mathrm{I}_{2\ell}\otimes 0_{2r}$ can not have more than 2ℓ eigenvalues with absolute values exceeding 1.

Property (a) is a consequence of G being the correlation matrix of a positive semidefinite Gaussian. Property (b) can be proved as follows: Let $\vec{w}$ a normalized vector with $w_i=0$ for any $i\leqslant 2\ell$. Then

$$\vec{w}^\dagger(G+i\mathrm{I}_{2\ell}\otimes 0_{2r})^\dagger(G+i\mathrm{I}_{2\ell}\otimes 0_{2r})\vec{w}=\vec{w}^\dagger G^2\vec{w}\leqslant 1, \quad \text{(B20)}$$

where the inequality follows from property (a). If there were more than 2ℓ eigenvalues λ of $G+i\mathrm{I}_{2\ell}\otimes 0_{2r}$ with modulus larger than 1, we could find a linear combination $\vec{W}=\sum_i c_i\vec{v}_i$ of the corresponding normalized eigenvectors $\vec{v}_i$ with the property $W_i=0$ for any $i\leqslant 2\ell$; this leads to a contradiction

with (B20) since

$$\sum_i c_i^* \vec{v}_i^\dagger (G + i\mathrm{I}_{2\ell}\otimes 0_{2r})^\dagger (G + i\ \mathrm{I}_{2\ell}\otimes 0_{2r}) \sum_j c_j \vec{v}_j$$
$$= \sum_i |c_i^2|\lambda_i^2 > \sum_i |c_i^2| = 1. \tag{B21}$$

This completes the proof of property (b).

Properties (a) and (b) imply that

$$|\det|G + i\mathrm{I}_{2\ell}\otimes 0_{2r}|| \leqslant 2^{2\ell}, \tag{B22}$$

which establishes that the determinants in (B18) remain finite in the limit $r\to\infty$. Concomitantly, the expression in Eq. (B18) approaches zero as $r\to\infty$. This establishes (B17). Putting everything together we see that (B16) can be written as

$$\|\rho_{\ell,o}\|_F = \lim_{r\to\infty} \frac{\sqrt{\det|\mathrm{I}_{2\ell}\oplus 0_{2r}\oplus \mathrm{I}_2 + i\Gamma_{A\cup B\cup n}|}}{2^{\frac{\ell}{2}+1}|m_\perp(t)|}, \tag{B23}$$

which is Eq. (11.25).

We stress that our assumption regarding the limit (B19) is equivalent to the existence of the limit in (B23). From a numerical point of view, this can be inferred from the scaling analysis of

$$\frac{\sqrt{\det|\mathrm{I}_{2\ell}\oplus 0_{2r}\oplus \mathrm{I}_2 + i\Gamma_{A\cup B\cup n}|}}{2^{\frac{\ell}{2}+1}|m_\perp(t)|}, \tag{B24}$$

which is still required to check the cluster decomposition hypothesis (see Fig. 11).

The magnetization $|m_\perp(t)|$ can be computed writing a self-consistent equation for Eq. (B23) in the case $\ell = 1$: From Eq. (11.19) we have

$$\|\rho_{1,o}\|_F = \sqrt{2}|m_\perp(t)|, \tag{B25}$$

which together with Eq. (B23) gives

$$4m_\perp^2(t) = \lim_{r\to\infty}\sqrt{\det(I_2\oplus 0_{2r}\oplus I_2 + i\Gamma_{1\cup B\cup n})}. \tag{B26}$$

APPENDIX C: CONSERVATION LAWS IN SPIN MODELS WITH FREE FERMION SPECTRA

In this Appendix we present a simple construction of the bulk contribution to local conservation laws of the TFIC on the infinite line. Our method readily generalizes to other models with free fermionic spectrum such as the XY chain. Ignoring boundary conditions, we can use the Jordan-Wigner transformation to express the Hamiltonian as a quadratic form in Majorana fermions

$$H = \frac{1}{2}\sum_{l,n} a_l \mathcal{H}_{ln} a_n. \tag{C1}$$

Here, $\mathcal{H}$ is a skew symmetric block-circulant matrix

$$\mathcal{H} = \begin{bmatrix} \mathcal{Y}_0 & \mathcal{Y}_1 & \dots & \mathcal{Y}_{L-1} \\ \mathcal{Y}_{L-1} & \mathcal{Y}_0 & & \vdots \\ \vdots & & \ddots & \vdots \\ \mathcal{Y}_1 & \dots & \dots & \mathcal{Y}_0 \end{bmatrix}, \tag{C2}$$

where $\mathcal{Y}_n = -\mathcal{Y}_{L-n}^T$ are 2×2 matrices. In Fourier space we have

$$(\mathcal{Y}_n)_{jj'} = \frac{1}{L}\sum_{k=1}^{L} e^{\frac{2\pi i k}{L}n}(Y_k)_{jj'}, \tag{C3}$$

where $(Y_k)_{jn} = -(Y_{-k})_{nj}$. One can show that a complete set of local conservation laws is obtained by taking

$$I_r = \frac{1}{2}\sum_{l,n} a_l \mathcal{I}_{r;ln} a_n. \tag{C4}$$

From Eq. (8.30) we see that $[H, I_r] = 0$ if and only if $[\mathcal{H},\mathcal{I}_r] = 0$. Similarly one has $[I_r, I_{r'}] = 0$ if and only if $[\mathcal{I}_r,\mathcal{I}_{r'}] = 0$. Hence the problem of constructing conservation laws is equivalent to determining an appropriate set of mutually commuting matrices that commute with $\mathcal{H}$. Because the projectors on the eigenvectors of block-circulant matrices are block-circulant matrices, we seek $\mathcal{I}_r$ in block-circulant form

$$\mathcal{I}_r = \begin{bmatrix} \bar{\mathcal{Y}}_0^{(r)} & \bar{\mathcal{Y}}_1^{(r)} & \dots & \bar{\mathcal{Y}}_{L-1}^{(r)} \\ \bar{\mathcal{Y}}_{L-1}^{(r)} & \bar{\mathcal{Y}}_0^{(r)} & & \vdots \\ \vdots & & \ddots & \vdots \\ \bar{\mathcal{Y}}_1^{(r)} & \dots & \dots & \bar{\mathcal{Y}}_0^{(r)} \end{bmatrix}. \tag{C5}$$

Imposing $[\mathcal{H},\mathcal{I}_r] = 0$ and $[\mathcal{I}_r,\mathcal{I}_{r'}] = 0$ we obtain the conditions

$$\left[Y_k, \bar{Y}_k^{(r)}\right] = 0\,, \quad \left[\bar{Y}_k^{(r)}, \bar{Y}_k^{(r')}\right] = 0, \qquad \forall k \tag{C6}$$

where $\bar{Y}_k^{(r)}$ is the Fourier transform (C3) of $\bar{\mathcal{Y}}^{(r)}$. In the quantum Ising model Y_k are 2×2 traceless matrices, so Eq. (C6) has the simple solution

$$\bar{Y}_k^{(r)} = \omega_k^{(r)}\mathrm{I} + q_k^{(r)} Y_k, \tag{C7}$$

where $\omega_k^{(r)} = -\omega_{-k}^{(r)}$ and $q_k^{(r)} = q_{-k}^{(r)}$. Fourier transforming back to position space we have

$$\bar{\mathcal{Y}}_n^{(r)} = \frac{1}{L}\sum_{k=1}^{L} e^{\frac{2\pi i k}{L}n}\omega_k^{(r)}\mathrm{I} + \frac{1}{L}\sum_{k=1}^{L} e^{\frac{2\pi i k}{L}n} q_k^{(r)} Y_k. \tag{C8}$$

We define the "range" of a local conservation as the maximal number of neighboring spins involved in its density minus one. By construction, the range is equal to the maximal $|n|$ such that $\bar{\mathcal{Y}}_n^{(r)}$ is nonzero [cf. Eqs. (C1) and (C2)]. For the TFIC one finds that $Y_n = 0$ for $|n| > 1$, and concomitantly the range of the Hamiltonian is $r_H = 1$. It is straightforward to identify the conservation laws with ranges $\leqslant r+1$: from Eq. (C8) they are such that

$$\omega_k = \sum_{n=1}^{r+1} c_n^- \sin(nk)\,, \qquad q_k = \sum_{n=0}^{r+1-r_H} c_n^+ \cos(nk). \tag{C9}$$

They can be divided in two classes: one with $q_k = 0$, which we denote by I^-, and one with $\omega_k = 0$, which we denote by

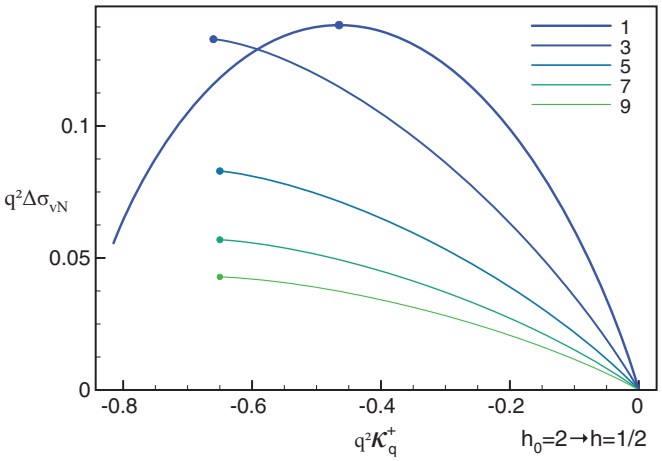

FIG. 20. (Color online) The difference of entanglement entropy densities $\Delta\sigma_{vN} = \sigma_{vN}^{\mathrm{dGGE}(+q)} - \sigma_{vN}^{\mathrm{GGE}}$ as a function of the parameter κ_q^+ for the same quench shown in Fig. 9 (the legend indicates the value of q). The points have the maximal entropy and correspond to the lines plotted in Fig. 9. Only for $q = 1$ is the entanglement entropy maximal at a stationary point.

I^+. Finally, a complete set of conservation laws is given by

$$I_r^+ : \bar{\mathcal{Y}}_n^{+,(r)} = \frac{1}{L}\sum_{k=1}^{L} e^{\frac{2\pi i k}{L}n}\cos(rk)Y_k,$$
$$I_r^- : \bar{\mathcal{Y}}_n^{-,(r)} = -\frac{2J}{L}\sum_{k=1}^{L} e^{\frac{2\pi i k}{L}n}\sin[(r+1)k]\mathrm{I}. \tag{C10}$$

These are exactly the conservation laws reported in Eq. (2.13).

We note that the conservation laws I_r^- are independent of the system details, and can be found in any noninteracting model with a block-circulant structure (see also Ref. 59). Indeed they are originated from the trivial solution of Eq. (C6), namely, the identity.

APPENDIX D: PECULIAR ASPECTS OF DEFECTIVE GGEs

In this Appendix we discuss some properties of the defective generalized Gibbs ensembles defined in Sec. VI. We start by recalling the standard variational approach for deriving statistical ensembles in quantum mechanics. One generally seeks the density matrix that maximizes the entropy under a given set of constraints on independent, additive conservation laws I_j:

$$\delta\,\mathrm{Tr}\Big[-\rho\,\ln\rho - \lambda\rho - \sum_j \lambda_j I_j \rho\Big] = 0. \tag{D1}$$

The solution of (D1) is of the form $\rho \propto \exp(\sum_j \lambda_j I_j)$, which shows that the ensemble is a function only of the conservation laws appearing in Eq. (D1).

We now consider the density matrix after a quench. All the ensembles defined in the main text are compatible with the principle of maximal entanglement entropy, and the GGE, the truncated GGE, and the truncated defective GGE can be obtained (*a posteriori*) by means of the variational approach (D1).

Some complications arise when we consider defective GGEs, in which we exclude a single integral of motion. From Eq. (6.5) we find that the entanglement entropy density $\sigma_{\mathrm{vN}}^{\mathrm{dGGE}(+q)}$ of the defective GGE $\rho_{\mathrm{dGGE}}^{(+q)}$ (Ref. 70) is given by

$$\sigma_{\mathrm{vN}}^{\mathrm{dGGE(+q)}} = \int_0^\pi \frac{dk}{\pi} H\left(\cos\Delta_k - \kappa_q^+ \frac{\cos(qk)}{\varepsilon(k)}\right), \tag{D2}$$

where $H(x) = -\frac{1+x}{2}\ln\frac{1+x}{2} - \frac{1-x}{2}\ln\frac{1-x}{2}$. By writing the defective GGE as in Eq. (4.2), one can easily show that $\frac{\partial\sigma_{\mathrm{vN}}^{\mathrm{dGGE(+q)}}}{\partial k_q^+}$ is the Lagrange multiplier associated to the conservation law I_q^+ [cf. Eq. (4.5)]: if the maximum of the entanglement entropy is not at the boundaries of the domain of k_q^+, then the equation $\frac{\partial\sigma_{\mathrm{vN}}^{\mathrm{dGGE(+q)}}}{\partial k_q^+} = 0$ has a solution, and $\rho_{\mathrm{dGGE}}^{(+q)}$ can be obtained from Eq. (D1). In the absence of peculiar constraints, one would expect the maximum to be generally a stationary point of the entanglement entropy. However, quenches in translationally invariant noninteracting models are very special since the initial state is a simultaneous eigenstate of an infinite number of local conservation laws. This substantially reduces the degrees of freedom, and can result in an exceptionally small domain for k_q^+ (which may not include a stationary point). In Fig. 20 we show this paradoxical behavior for the same set of parameters used in Fig. 9. Besides the pathological cases of even q, in which the curves collapse to the point $\kappa_q^+ = 0$, the effect of the reduction of degrees of freedom is reflected in the "truncated" shape of the curves for $q \neq 1$, which turn out to be strictly decreasing functions of κ_q^+. The limiting procedure (6.2) selects the value of κ_q^+ corresponding to the maximal entanglement entropy (the circles in Fig. 20).

[1] M. Greiner, O. Mandel, T. W. Hänsch, and I. Bloch, Nature (London) **419**, 51 (2002).
[2] T. Kinoshita, T. Wenger, and D. S. Weiss, Nature (London) **440**, 900 (2006).
[3] S. Hofferberth, I. Lesanovsky, B. Fischer, T. Schumm, and J. Schmiedmayer, Nature (London) **449**, 324 (2007).
[4] S. Trotzky, Y.-A. Chen, A. Flesch, I. P. McCulloch, U. Schollwöck, J. Eisert, and I. Bloch, Nat. Phys. **8**, 325 (2012).
[5] M. Cheneau, P. Barmettler, D. Poletti, M. Endres, P. Schauss, T. Fukuhara, C. Gross, I. Bloch, C. Kollath, and S. Kuhr, Nature (London) **481**, 484 (2012).
[6] M. Gring, M. Kuhnert, T. Langen, T. Kitagawa, B. Rauer, M. Schreitl, I. Mazets, D. Adu Smith, E. Demler, and J. Schmiedmayer, Science **337**, 1318 (2012).
[7] A. Polkovnikov, K. Sengupta, A. Silva, and M. Vengalattore, Rev. Mod. Phys. **83**, 863 (2011).
[8] M. Rigol, V. Dunjko, V. Yurovsky, and M. Olshanii, Phys. Rev. Lett. **98**, 050405 (2007); A. C. Cassidy, C. W. Clark, and M. Rigol, *ibid.* **106**, 140405 (2011).
[9] M. Rigol, V. Dunjko, and M. Olshanii, Nature (London) **452**, 854 (2008).
[10] P. Calabrese and J. Cardy, J. Stat. Mech. (2007) P06008.

[11] V. Gritsev, E. Demler, M. Lukin, and A. Polkovnikov, Phys. Rev. Lett. **99**, 200404 (2007).

[12] M. A. Cazalilla, Phys. Rev. Lett. **97**, 156403 (2006); A. Iucci and M. A. Cazalilla, Phys. Rev. A **80**, 063619 (2009).

[13] T. Barthel and U. Schollwöck, Phys. Rev. Lett. **100**, 100601 (2008).

[14] D. Rossini, A. Silva, G. Mussardo, and G. Santoro, Phys. Rev. Lett. **102**, 127204 (2009); D. Rossini, S. Suzuki, G. Mussardo, G. E. Santoro, and A. Silva, Phys. Rev. B **82**, 144302 (2010).

[15] A. Silva, Phys. Rev. Lett. **101**, 120603 (2008).

[16] S. R. Manmana, S. Wessel, R. M. Noack, and A. Muramatsu, Phys. Rev. B **79**, 155104 (2009).

[17] M. Moeckel and S. Kehrein, Ann. Phys. (NY) **324**, 2146 (2009).

[18] D. Fioretto and G. Mussardo, New J. Phys. **12**, 055015 (2010).

[19] G. Biroli, C. Kollath, and A. M. Läuchli, Phys. Rev. Lett. **105**, 250401 (2010).

[20] M. C. Bañuls, J. I. Cirac, and M. B. Hastings, Phys. Rev. Lett. **106**, 050405 (2011).

[21] C. Gogolin, M. P. Müller, and J. Eisert, Phys. Rev. Lett. **106**, 040401 (2011).

[22] J. Mossel and J.-S. Caux, New J. Phys. **12**, 055028 (2010).

[23] P. Barmettler, M. Punk, V. Gritsev, E. Demler, and E. Altman, New J. Phys. **12**, 055017 (2010).

[24] P. Calabrese, F. H. L. Essler, and M. Fagotti, Phys. Rev. Lett. **106**, 227203 (2011).

[25] M. Rigol and M. Fitzpatrick, Phys. Rev. A **84**, 033640 (2011).

[26] S. Sotiriadis, D. Fioretto, and G. Mussardo, J. Stat. Mech. (2012) P02017.

[27] M. A. Cazalilla, A. Iucci, and M.-C. Chung, Phys. Rev. E **85**, 011133 (2012).

[28] A. Mitra and T. Giamarchi, Phys. Rev. Lett. **107**, 150602 (2011).

[29] F. Iglói and H. Rieger, Phys. Rev. Lett. **85**, 3233 (2000); H. Rieger and F. Iglói, Phys. Rev. B **84**, 165117 (2011); F. Iglói and H. Rieger, Phys. Rev. Lett. **106**, 035701 (2011).

[30] D. Schuricht and F. H. L. Essler, J. Stat. Mech. (2012) P04017.

[31] P. Calabrese, F. H. L. Essler, and M. Fagotti, J. Stat. Mech. (2012) P07016.

[32] P. Calabrese, F. H. L. Essler, and M. Fagotti, J. Stat. Mech. (2012) P07022.

[33] J. Mossel and J.-S. Caux, New J. Phys. **14**, 075006 (2012).

[34] J.-S. Caux and R. M. Konik, Phys. Rev. Lett. **109**, 175301 (2012).

[35] L. Foini, L. F. Cugliandolo, and A. Gambassi, J. Stat. Mech. (2012) P09011.

[36] F. H. L. Essler, Stefano Evangelisti, and M. Fagotti, Phys. Rev. Lett. **109**, 247206 (2012).

[37] G. P. Brandino, A. De Luca, R. M. Konik, and G. Mussardo, Phys. Rev. B **85**, 214435 (2012).

[38] J. Marino and A. Silva, Phys. Rev. B **86**, 060408 (2012).

[39] C. Gramsch and M. Rigol, Phys. Rev. A **86**, 053615 (2012).

[40] C. Karrasch, J. Rentrop, D. Schuricht, and V. Meden, Phys. Rev. Lett. **109**, 126406 (2012).

[41] J. Rentrop, D. Schuricht, and V. Meden, New J. Phys. **14**, 075001 (2012).

[42] M. Heyl, A. Polkovnikov, and S. Kehrein, Phys. Rev. Lett. **110**, 135704 (2013).

[43] E. Demler and A. M. Tsvelik, Phys. Rev. B **86**, 115448 (2012).

[44] M. Cramer, C. M. Dawson, J. Eisert, and T. J. Osborne, Phys. Rev. Lett. **100**, 030602 (2008).

[45] M. Cramer and J. Eisert, New J. Phys. **12**, 055020 (2010).

[46] J. M. Deutsch, Phys. Rev. A **43**, 2046 (1991); M. Srednicki, Phys. Rev. E **50**, 888 (1994); J. Phys. A **29**, L75 (1996); **32**, 1163 (1999); M. Rigol and M. Srednicki, Phys. Rev. Lett. **108**, 110601 (2012).

[47] We have in mind regularizing the system by enclosing it in a very large but finite volume.

[48] M. Olshanii, arXiv:1208.0582.

[49] See, e.g., S. Sachdev, *Quantum Phase Transitions* (Cambridge University Press, Cambridge, UK, 2011).

[50] E. Barouch, B. McCoy, and M. Dresden, Phys. Rev. A **2**, 1075 (1970).

[51] Y.-A. Chen, S. Nascimbène, M. Aidelsburger, M. Atala, S. Trotzky, and I. Bloch, Phys. Rev. Lett. **107**, 210405 (2011).

[52] O. Viehmann, J. von Delft, and F. Marquardt, Phys. Rev. Lett. **110**, 030601 (2013); New J. Phys. **15**, 035013 (2013).

[53] T. Prosen, J. Phys. A **31**, L397 (1998); M. Grady, Phys. Rev. D **25**, 1103 (1982).

[54] J. Lancaster and A. Mitra, Phys. Rev. E **81**, 061134 (2010).

[55] T. Caneva, E. Canovi, D. Rossini, G. E. Santoro, and A. Silva, J. Stat. Mech. (2011) P07015.

[56] F. H. L. Essler and R. M. Konik, *Ian Kogan Memorial Collection: From Fields to Strings: Circumnavigating Theoretical Physics*, edited by M. Shifman, A. Vainshtein, and J. Wheater (World Scientific, Singapore, 2005).

[57] G. Mussardo, *Statistical Field Theory, An Introduction to Exactly Solved Models in Statistical Physics* (Oxford University Press, Oxford, UK, 2009).

[58] G. Mussardo (private communication).

[59] M. Fagotti, Phys. Rev. B **87**, 165106 (2013).

[60] M. Fagotti and P. Calabrese, J. Stat. Mech. (2010) P04016.

[61] M. Fagotti, Europhys. Lett. **97**, 17007 (2012).

[62] I. Peschel and V. Eisler, J. Phys. A **42**, 504003 (2009).

[63] It is also known as the "Hilbert-Schmidt norm," but we prefer to call it "Frobenius norm" to emphasize that we are considering finite subsystems.

[64] We have not proven that $\mathcal{D}(\rho,\rho')$ obeys the triangle inequality as this is not essential for our purposes.

[65] G. Vidal, J. I. Latorre, E. Rico, and A. Kitaev, Phys. Rev. Lett. **90**, 227902 (2003); J. I. Latorre, E. Rico, and G. Vidal, Quant. Inf. Comput. **4**, 048 (2004); B-Q. Jin and V. E. Korepin, J. Stat. Phys. **116**, 79 (2004).

[66] M. Fagotti and P. Calabrese, Phys. Rev. A **78**, 010306(R) (2008).

[67] P. Calabrese and J. Cardy, J. Stat. Mech. (2005) P04010.

[68] A. Wehrl, Rev. Mod. Phys. **50**, 221 (1978).

[69] Kh. D. Ikramov and H. Fassbender, J. Math. Sci. **157**, 697 (2009).

[70] This is defined as the limit $L \to \infty$ of the finite volume entropy density $\sigma_{\rm vN}^{\rm dGGE(+q)} = \lim_{L\to\infty} \frac{1}{L} S_{\rm vN}^{\rm dGGE(+q)}$.